UNIVERSITÀ DEGLI STUDI DI SASSARI

CORSO DI DOTTORATO DI RICERCA IN SCIENZE BIOMEDICHE

Coordinatore del Corso: Prof. Andrea Fausto Piana

CURRICULUM IN ONCOLOGIA MOLECOLARE

Responsabile di Curriculum: Prof.ssa Rosa Maria Pascale

XXIX CICLO

Identification and characterization of cytogenetic profile in olfactory neuroblastoma by array comparative genomic hybridization

Coordinatore:

Prof. Andrea Fausto Piana

Tutor:

Prof. Francesco Meloni

Prof.ssa Rosa Maria Pascale

Tesi di dottorato di:

Dott. Luca Volpi

Anno Accademico 2015 – 2016

CONTENTS

1. INTRODUCTION **6**

2. OLFACTORY NEUROBLASTOMA **7**

2.1 Clinical features 7

2.2 Imaging Studies 9

2.3 Staging system 10

2.4 Histology 11

2.5 Treatment and results 14

2.6 Surgery 15

2.7 Radiotherapy 17

2.8 Chemotherapy 18

3. ARRAY COMPARATIVE GENOMIC HYBRIDIZATION **19**

3.1 a-CGH definition and technique 19

3.2 Principles and research applications of Array CGH 21

3.3 a-CGH and olfactory neuroblastoma 23

4. MATHERIALS AND METHODS **28**

4.1 Patients 28

4.2 Hystological method 29

4.3 Technique of a-CGH 31

5. RESULTS **47**

5.1 Clinical results 47

5.2 Hystopatological results 48

5.3 a-CGH results 49

6. DISCUSSION **65**

7. REFERENCES **69**

FIGURES INDEX

Figure 1: Endoscopic view of olfactory neuroblastoma 8
Figure 2: MR- aspects of ONB 9
Figure 3: Schematic representation of CGH microarray technology 20
Figure 4: copy number aberrations in ONBs in Guled's paper 27
Figure 5: histological features of ONB 30
Figure 6: a-CGH workflow diagram for sample preparation and microarray processing..... 32
Figure 7: Slide in slide holder for SureScan microarray scanner..... 43
Figure 8: Agilent scanner 46
Figure 9: histologic features of ONB 33
Figure 10: a-CGH workflow 35
Figure 11: Slide in slide holder for SureScan microarray scanner..... 43
Figure 12: agilent scanner 46
Figure 13: percentage of patients with DNA gain or loss for each chromosome 52
Figure 14: chromosomal gains 53
Figure 15: chromosomal loss 54
Figure 16: percentage of patients with DNA gain or loss for each chromosome (FRESH) 55
Figure 17: percentage of patients with DNA gain or loss for each chromosome (FFPE). 58
Figure 18: chromosome 1 FFPE vs FRESH 63
Figure 19: chromosome 1 FFPE vs FRESH: scattered plot profile..... 63
Figure 20: chromosome 20 FFPE vs FRESH..... 64
Figure 21: chromosome 5 ffpe vs FRESH 64

TABLES INDEX

Table 1: Kadish staging system.....10
Table 2: Dulguerov and Calcaterra staging system.....10
Table 3: Hyams' grading system.....12
Table 4: Immunohistochemical features of olfactory neuroblastoma.....13
Table 5: Features for differential diagnosis…...…….13
Table 6:Olfactory neuroblastoma: comparison of survival results (1992 – 2008) according to Devaiah's meta-analysis……...……..16
Table 7: Median Follow-up Times (months) for olfactory neuroblastoma……17
Table 8: Most common alterations in ONB found in Bockmuhl's paper……..……24
Table 9: cytogenetic features showed in Holland's paper…….…….25
Table 10: Clinical data on olfactory neuroblastomas (personal case-series)…….28
Table 11: amplificated regions for patient and for chromosomes showed by the a-CGH.....50
Table 12: loss regions for patients and for chromosomes showed by the a-CGH.....51
Table 13: amplificated regions in fresh tissue samples showed by the a-CGH.....56
Table 14: loss regions in fresh tissue samples showed by the a-CGH.....57
Table 15: amplificated regions in FFPE tissue samples showed by the a-CGH.....59
Table 16: loss regions in FFPE tissue samples showed by the a-CGH ……..…. 60

1. INTRODUCTION

Olfactory neuroblastoma (ONB) is a rare malignant neoplasm arising from the olfactory neuroepithelium[1,2]. Its incidence is 0.4 patients per million per year, and it represents about 3% of malignant tumours of the nasal cavity and paranasal sinuses[3,4]. Basal cells of the olfactory neuroepithelium are presumably the progenitors of the ONB. The neoplasm usually arises in the olfactory vault of the nasal fossa and it is intimately related to the cribriform plate. Often, diagnosis is made late because early stage ONBs are usually asymptomatic. The incidence of cervical metastasis varies from 5 to 12% at the time of diagnosis, whereas distant metastases occur in 12 to 25% of patients. To date, no universally accepted classification systems have been adopted; the Hyams' grading system is usually used to histologically grade the tumors and the Kadish system is used to stage them[5,6].

Cytogenetic data on ONB are scarce; in one study by Guled et al. (2008) the authors analysed tumor samples from 13 patients by array comparative genomic hybridization (a-CGH). The authors observed a number of recurrent chromosome region gains and losses, which might also be related to the tumor stage. In particular, gains of 20q and 13q were suggested to be important in cancer progression[7]. Here we present data on 13 DNA samples from12 patients with ONB analyzed by a-CGH. The aim of our study was to better define the cytogenetic profile of ONB by a-CGH, and identify possible correlations with clinical and pathological features, evaluating the advantages and limits of the technique.

The analyzed patients were treated at the Department of Otolaryngology of Varese and followed

with a careful follow-up. At the Department of Pathology tumor samples of the patients were reviewed with the use of immunohistochemical techniques to confirm the diagnosis of ONB. At the Section of Biology and Medical Genetics, Department of Clinical and Experimental Medicine of Varese, the DNA analysis of tumors were carried out using a-CGH technique.

2. OLFACTORY NEUROBLASTOMA

Olfactory neuroblastoma (ONB) is an uncomm malignant neuroectodermal nasal tumour. ONBs are thought to arise from the specialized sensory neuroepithelial (neuroectodermal) olfactory cells that are normally found in the upper part of the nasal cavity, including the superior nasal concha, the upper part of septum, the roof of nose, and the cribriform plate of ethmoid[8].

2.1 Clinical features

Those tumors usually present with unilateral nasal obstruction and epistaxis. Impairment or loss of the sense of smell is not common as a clinical symptom as might be expected, in part because olfaction is preserved on the contra lateral side in some tumors and in part because some patients fail to notice its gradual loss. Extension into the intracranial cavity rarely causes neurological symptoms as invasion of the frontal lobe only produces symptoms after massive involvement. Large tumors can invade the orbit and produce ocular symptoms.

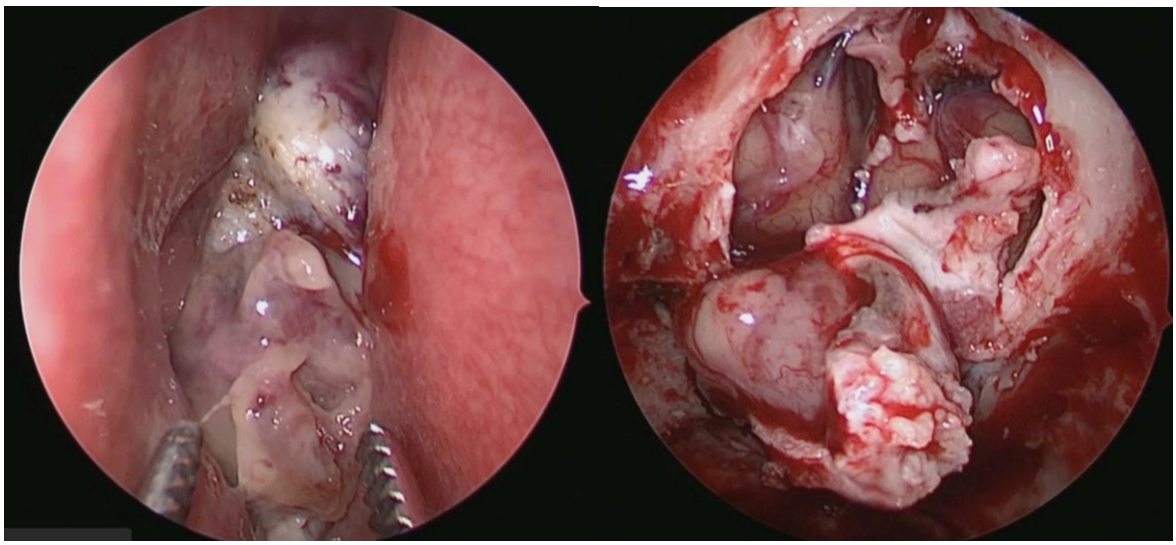

Figure 1: Endoscopic view of olfactory neuroblastoma

2.2 Imaging Studies

The imaging features of olfactory neuroblastoma are non-specific. Nevertheless, this neoplasm should be suspected when a mass is detected in the superior nasal cavity, causing either remodeling or destruction of adjacent bony structures, and erosion of the cribriform plate or of the fovea ethmoidalis[9].

The stage at initial presentation is highly predictive of survival and accurate staging is essential. Appropriate evaluation includes both computed tomography (CT) and magnetic resonance imaging (MRI), to help define the likely extent of the disease both at the primary site and in the neck. However, thosee imaging modalities are complimentary and should be performed in all cases. Fine-cut spiral overlapping CT scan in all three dimensions is the radiological study of choice.

Olfactory neuroblastoma does not have any specific radiological appearance but its site in the olfactory cleft makes it a likely diagnosis in its early stages. It is seen is a homogenous soft-tissue mass in the nasal vault, with uniform and moderate contrast enhancement and occasionally the adjacent bone can be hyperostotic. CT images are essential for correct staging and should be carefully examined for erosion of the lamina papryacea, cribriform plate, and fovea ethmoidalis. MRI enables a better estimate of tumor spread into surrounding soft tissue and areas in particular it can indicate whether the tumor has involved or traversed the dura and/or the orbit and can differentiate mucus from tumor[10].

.

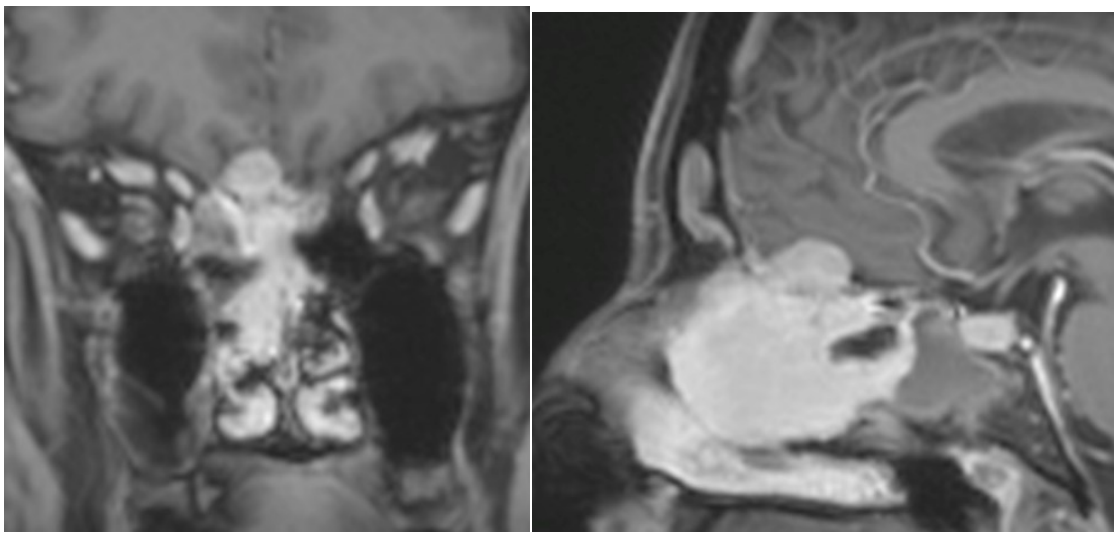

a **b**

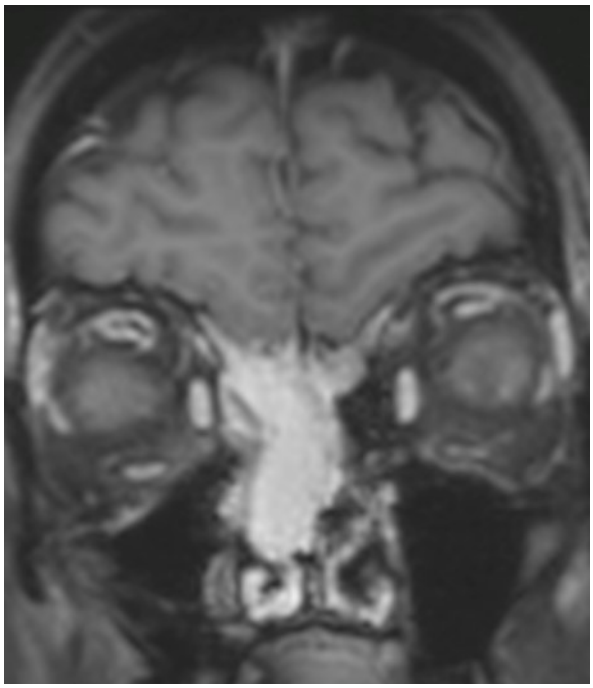

c

Figure 2: MR - aspects of ONB

a. Coronal MR T1 with contrast shows a mass with a low- to intermediate signal, epicenter within the right ethmoid and intracranial extension. **b** On sagittal plane post contrast MR demonstrates that the tumor extends into the anterior cranial fossa **c.** A post contrast coronal MR of a case without intracranial spread into the anterior cranial fossa

2.3 Staging system

Different staging systems based on the extension of the lesion[11] have been specifically proposed for olfactory neuroblastoma (Table 1 and 2).

Table 1: Kadish staging system

Kadish staging system (1976)

Stage	Features
A	Tumor confined to the nasal cavity
B	Tumor confined to the nasal cavity, involving one or more paranasal sinuses
C	Tumor extending beyond the nasal cavity and paranasal sinuses. Includes involving of the orbit, skull base, intracranial cavity, cervical lymph nodes and distant metastatic sites

Table 2: Dulguerov and Calcaterra staging system

Dulguerov and Calcaterra staging system (1992)

Stage	Features
T1	Tumor involving the nasal cavity and/or paranasal sinuses, sparing the most superior ethmoidal cells
T2	Tumor involving the nasal cavity and/or paranasal sinuses, including the sphenoid, with extension to and erosion of the cribriform plate
T3	Tumor extending into the orbit or protruding into the anterior cranial fossa
T4	Tumor involving the brain

Kadish and co-workers[11] were the first to propose a staging classification, using three categories, Group A, B and C (Table1). A further system was proposed with the advent of advances in imaging (241), based on the TNM system (Table 2). Although a system of classification has been proposed, various attempts have been made to modify the Kadish system[11,12]. Other authors suggest that by

using the Kadish staging system and the Hyams grading system independently they can predict patients outcome with more accuracy[13]. Hyams grading system is based on histology and will be referred in the next section.

2.4 Histology

Olfactory neuroblastoma is an uncommon sinonasal tumour, and can often been confused with other neoplasms, e.g. sinonasal undifferentiated carcinoma, neuroendocrine carcinoma, melanoma, lymphoma, plasmacytoma, embryonal rhabdomyosarcoma, Ewing's sarcoma, peripheral primitive neuroectodermal tumours, vascular tumours etc.. It was this frustrating feature that prompted Ogura and Schenek[14] to describe olfactory neuroblastoma as the "great impostor". The diagnosis of olfactory neuroblastoma can be problematic and consequently, histochemical, immunochemical and ultrastructural investigations are often needed to support the diagnosis[15]. Westra and colleagues from Johns Hopkins reviewed 37 cases of diagnosed olfactory neuroblastoma and excluded 8 (21.6%) because they did not meet diagnostic inclusion criteria[16]. Hirose et al.[15] from the Mayo Clinic Tissue Registry reviewed 30 cases of olfactory neuroblastoma and found that 4 (13.3%) were excluded because they lacked neural or neuroendocrine markers. Exhibiting only epithelial markers, they were considered examples of sinonasal undifferentiated carcinoma.

It is reported that a diagnosis of olfactory neuroblastoma by light microscopy is not difficult when the tumor is well differentiated and consists of homogenous small cells with uniform round to oval nuclei, with rosette or pseudorosette formation, and eosinophilic fibrillary intercellular background material. Hyams et al.[17] proposed a grading system for olfactory neuroblastoma, Grades I being well differentiated to IV undifferentiated, based on several tumour histological parameters: preservation of lobular architecture, mitotic index, nuclear polymorphism, fibrillary matrix, the presence of HW (Horner Wright) or FW (Flexner-Wintersteiner) rosettes, and the presence or absence of tumour necrosis.

Table 3: Hyams' grading system

Olfactory neuroblastoma grading (based on Hyams' grading system)

Microscopic features	Grade I	Grade II	Grade III	Grade IV
Architecture	Lobular	Lobular	±Lobular	±Lobular
NF matrix	Prominent	Present	May be present	Present
Rosettes	HR	HR	FW	FW
Mitoses	Absent	Present	Prominent	Marked
Necrosis	Absent	Absent	Present	Prominent
Glands	May be present	May be present	May be present	May be present
Calcification	Variable	Variable	Absent	Absent

NF neurofibrillary, *HR* Homer Wright pseudorosettes, *FW* Flexner-Wintersteiner rosettes

When the tumor is undifferentiated with anaplastic hyperchromatic small cells that show many mitotic figures and scant cytoplasm, differentiating the tumor from other small-cell nasal neoplasms by light microscopy becomes difficult. To summarise, the pathologic distinction of poorly differentiated small cell neoplasms of the nasal cavity is difficult and can only be based on the results of antigen expression using a panel of antibodies by immunohistochemistry and if necessary confirmed by electron microscopy. There is still a lack of consensus relating to these prognostic histological features. Support for the prognostic value of Hyams and co-workers grading[17] has been published[18]. Histopathological staging according to Hyams has also been advocated more recently in predicting survival and prognosis[19]. Hirose and colleagues found that a high degree of S-100

immunopositivity and a low (<10%) Ki-67 labelled index (a marker for proliferation) was associated with better survival. There are conflicting data on the prognostic role of p53 tumor suppressor gene mutations[13] .

Table 4: Immunohistochemical features of olfactory neuroblastoma

positive	negative
neuron specific enolase (NSE) synaptophysin cromogranine A S-100 neurofilament protein (NFP)	Cytokeratin epithelial membrane antigen (EMA) carcinoembryonic antigen (CEA) CD45 CD99 HMB45 Melan A Desmin

Table 5: Features for differential diagnosis

Feature	**Olfactory neuroblastoma**	**Sinonasal undifferentiated carcinoma**	**Ewing sarcoma/PNET**	**Neuroendocrine carcinoma**
Mean age	40–45 years	55–60 years	<30 years	50 years
Site	Roof of nasal cavity	Multiple sites usually	Maxillary sinus > nasal cavity	Superior/posterior nasal cavity, ethmoid, maxillary sinuses
Imaging studies	"Dumbbell-shaped" cribriform plate mass	Marked destruction/spread	Mass lesion with bone erosion	May invade skull base or orbit
Prognosis	60–80% 5-year survival	<20% 5-year survival	60–70% 5-year (stage, size, *FLI1*)	>60% die of disease
Cranial nerve	Sometimes	Common	Sometimes	Uncommon

Feature	Olfactory neuroblastoma	Sinonasal undifferentiated carcinoma	Ewing sarcoma/PNET	Neuroendocrine carcinoma
involvement				
Pattern	Lobular	Sheets and nests	Sheets, nests	Ribbons, islands
Cytology	Salt and pepper chromatin, small nucleoli (grade dependent)	Medium cells, inconspicuous nucleoli	Medium, round cells, vacuolated cytoplasm, fine chromatin	Salt and pepper, granular chromatin
Anaplasia	Occasionally and focally	Common	Minimal	Moderate
Mitotic figures	Variable	High	Common	High
Necrosis	Occasionally	Prominent	Frequent	Prominent
Vascular invasion	Occasionally	Prominent	Rare	Present
Neurofibrillary stroma	Common	Absent	Absent	Absent
Pseudorosettes	Common	Absent	Present	Present
Keratin	Focal, weak	>90%	Rare	Positive
CK 5/6	Negative	Negative	n/a	n/a
EMA	Negative	50%	n/a	n/a
NSE	>90%	50%	Positive	Positive
S-100 protein	+ (sustentacular)	<15%	Rare	Positive
Synaptophysin	>90% (can be weak)	<15%	Positive	Positive
In situ EBER	Absent	Absent	Absent	Absent
Neurosecretory granules (EM)	Numerous	Rare	Absent	Present

EBER Epstein barr virus encoded RNA (EBV-encoded RNA)

Modified From: Thompson 2009

2.5 Treatment and results

The Primary Site

A combination of surgery and radiotherapy is the most frequently used approach, and the one that achieved the highest cure rates[20]. Despite the lack of support for single-modality treatment regimes[21], a substantial number of patients are treated by surgery or radiotherapy alone. The difference in survival between the combined treatments and radiotherapy alone is significant. The 5-year disease-specific survival in the literature is reported between 52–90%[1]. Surgery alone was associated with lower survival combined with a combination of radiotherapy and chemotherapy, or triple modality treatment (surgery, radiotherapy and chemotherapy). Although the results were 15-20% better, the differences from the best combination were not statistically significant, probably because of the limited number of patients[2]. These results were complied from the MEDLINE database from 1990–2000, without language tags. There were 26 treatment studies that formed the basis for the above tabulations and data extracted from these studies comprised the total number of patients, the staging system used, the patients' distributions by stage and the histological grade and the treatment used. Outcome data consisted of recurrence free survival at 3 years and 5 years, overall survival at 5 and 10 years, and the results by stage, grade and treatment modality. In five studies, olfactory neuroblastoma were histo-pathologically graded according to Hyams et al., the mean 5 year survival was 56% in patients with grades I or II tumours and 25% in those with tumours of grade III or IV. This difference was significant (odds ration 6.18 {95% CI 1.30 – 29.3}). In 25 studies that used the Kadish classification, the mean 5 year survival for these three groups was Group A 72%, Group B 59% and Group C 47%, respectively. On average, 5% (SD 7) of patients presented with cervical lymph node metastases. In the studies of survival data according to N stage, only 29% of N+ patients were treated successfully, compared with 64% of N0, a significant difference (Odds ratio 5.1 {95% CI 1.6 – 17.0}).

2.6 Surgery

Most institutions favour surgery as the first treatment modality, followed by radiotherapy[22,23,24]. Endocranial extension and a close relation to the ethmoid roof and cribriform plate have conventionally led to a combined transfacial and neurosurgical approach. Craniofacial resection allows for an en bloc resection of the tumour with better assessment of any intracranial extension and protection of the brain and optic nerve. The resection should include the entire cribriform plate and crista galli. It is said that the olfactory bulb and overlying dura should be removed with the specimen although there is no clear evidence to support the assertion that the whole of the bulb should be removed[25]. Open surgery has long been regarded as the gold standard, with results available for decades. A craniotomy is probably not justified for T1 tumours where there is clear radiological evidence of a normal cribriform plate and no involvement of the upper ethmoidal cells although this clinical picture is seldom seen. The evolution of surgical techniques has created another surgical option in the form of endoanasal endoscopic surgery. The use of endoscopic surgery for olfactory neuroblastoma followed by the use of the stereotactic radiosurgical gamma knife therapy has recently been used[26]. One report of 10 cases with a mean follow-up of 38 months used endoscopic resection alone without any recurrence although only 2 had Kadish stage C [27]. In the last decade, numerous articles with small numbers have been published on the endoscopic resection of olfactory neuroblastoma. Devaiah et al. reviewed the literature with a meta-analysis and showed that an endoscopic approach gave a better survival rate[28]. The aim of this study was to compare results of open, endoscopic, endoscopic-assisted, and nonsurgical treatments since the first publication that mentioned an endoscopic removal in the literature. This analysis extracted sufficient data in 361 subjects and the statistically significant results for the full cohort are summarized in Table 6.

Table 6: Olfactory neuroblastoma: comparison of survival results (1992 – 2008) according to Devaiah's meta-analysis

Treatment A	No	Treatment B	No	p-value
Open Surgery (endoscopic better)	145	Endoscopic surgery	40	0.0018
Open Surgery (endoscopic better)	145	Endoscopic assisted	57	0.0133

Endoscopic surgery produced overall better survival rates than open surgery with no significant difference between follow-up times in the endoscopic and open surgery groups (Table 7).

Table 7: Median Follow-up Times (months) for olfactory neuroblastoma

Open	51.0
Endoscopic	54.5
Endoscopic assisted	44.0
Nonsurgical	17.0

As the gold standard open procedure considerably predated endoscopic treatment, they also grouped the data according to the publication year. The endoscopic surgery group maintained better survival rates. This data shows evidence for the efficacy of endoscopic surgery in olfactory neuroblastoma. There are more cases of long-term follow-up in the open surgery group than the endoscopic treatment group and most of the open surgery tumors belonged to the Kadish C stage, whereas the endoscopic techniques were used more commonly for Kadish A and B tumors. This reflects how endoscopic surgery has mainly been used for less extensive lesions. This might not only be a

reflection of the size of the tumor but their pathology as more extensive lesions might be expected to be more invasive and less differentiated although this cannot be ascertained from the data available [28]. The most recent publication on endoscopic endonasal resection for all Kadish groups has just been published by Folbe et al. [29]. This is a retrospective, multicenter study with 23 patients operated endoscopically with postoperative radiotherapy in 16 patients. The mean follow-up was 45.2 months with one recurrence. The authors conclude that endoscopic surgery is replacing craniofacial resection and that oncologic control is not sacrificed when good endoscopic resection techniques are used.

2.6 Radiotherapy

Standard radiotherapeutic techniques include external megavoltage beam and a three-field technique; an anterior port is combined with wedge later fields to provide a homogeneous dose distribution. The doses range from 55 Gy to 65 Gy with the majority receiving above 60 Gy. Currently it is considered that radiotherapy should play a role in the management of olfactory neuroblastoma, particularly in patients who have had incomplete surgical resection or who present with residual disease . In a small retrospective series, a comparison was made between conventional radiotherapy and stereotactically guided conformal radiotherapy (SCRT). It was concluded that SCRT improved target coverage and sparing of organs at risk[30].

2.7 Chemotherapy

Olfactory neuroblastoma is regarded as a chemosensitive tumour based on multiple reported responses to treatment[31]. Neoadjuvant therapy is seldom curative on its own and it may be of no benefit in some patients. Individuals who respond to preoperative chemotherapy have a greater chance of long term disease-free surviva. It has been proposed that Hyams' grading is an important

predictor of response to chemotherapy[31], and it has been suggested that cisplatinbased chemotherapy is helpful in advanced, high-grade olfactory neuroblastoma and should be considered the choice in the systemic treatment of these patients.

Neoadjuvant chemotherapy has been advocated for patients with advanced disease at the University of Virginia over a 20 year period[32]. In thirty four consecutive patients, two thirds showed a significant reduction of tumour burden with adjuvant therapy and patients that showed a response to neoadjuvant therapy demonstrated a significantly larger disease- free mortality rate. Preoperative chemotherapy consisted of cyclophosphamide (650 mg/m2) and vincristine (1.5 mg/m2; maximal dose, 2 mg) there were administered every 3 weeks for 6 cycles. Adriamycin was used in combination with cyclosphosphamide in two patients. Most patients also received a total dose of 50 Gy of preoperative fractionatedradiation therapy.

3. ARRAY COMPARATIVE GENOMIC HYBRIDIZATION

3.1 a-CGH definition and technique

Chromosomal CGH was first introduced by Kallioniemi et al.[33] and has rerevolutionized cytogenetic studies over past decades. The precept of chromosomal CGH is competitive hybridization of equal amounts of test and normal genomic DNA onto metaphase chromosome spreads. Subsequent quantitative analysis delineates chromosomal aberration (gain or loss). A major limitation of this method, however, is its restricted resolution of 10-20 Mb[34].

This problem was overcome by the introduction of array CGH, in which a collection of mapped and annotated genomic clones replace metaphase chromosomes[35], allowing for higher resolution and identification of clones harbouring potential oncogenes and tumor suppressor genes.

The application of microarray-based comparative genomic hybridization (array CGH) to diagnostics is transforming the field of clinical cytogenetics. Array CGH compares DNA content from two differentially labeled genomes. The two genomes, a test (or patient) and a reference (or control), are cohybridized onto a solid support (usually a glass microscope slide) on which cloned or synthesized DNA fragments have been immobilized (Figure 3).

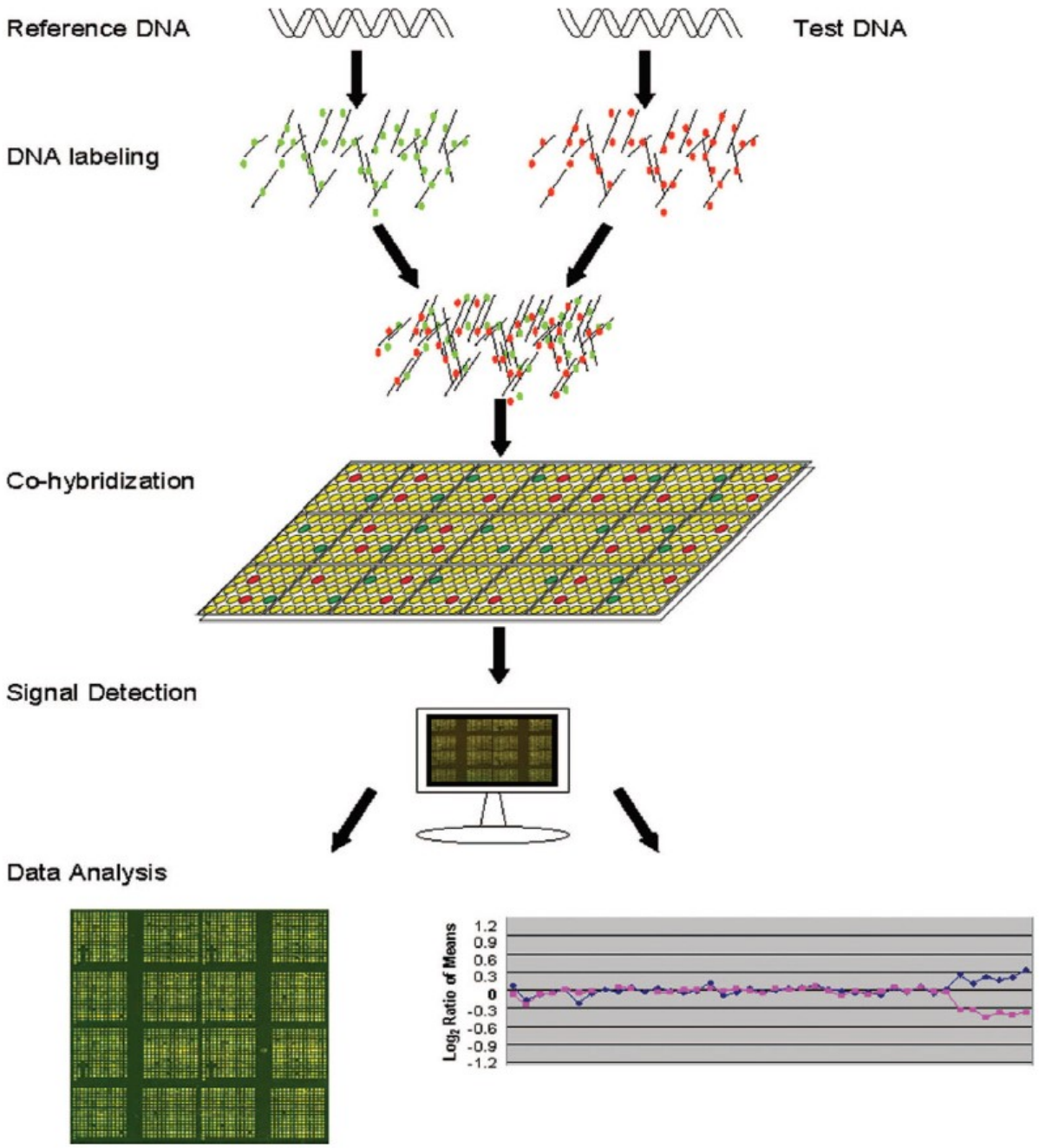

Figure 3. Schematic representation of CGH microarray technology. Whole genomic DNA from a control or reference (left) and genomic DNA from a test or patient (right) are differentially labeled with two different fluorophores. The two genomic DNA samples are competitively cohybridized with large-insert clone DNA targets that have been robotically printed onto the microarray (middle). Computer imaging programs assess the relative fluorescence levels of each DNA for each target on the array (lower left). The ratio between control and test DNA for each clone can be linearly plotted using data analysis software to visualize dosage variations (lower right), indicated by a deviation from the normal log2 ratio of zero.

Arrays have been built with a variety of DNA substrates that may include oligonucleotides, cDNAs, or bacterial artificial chromosomes (BACs). The resolution of the array is limited only by the size of the cloned DNA targets and the natural distance between these sequences located on the chromosome. The primary advantage of array CGH over fluorescence in situ hybridization (FISH) is the array's ability to detect DNA copy changes simultaneously at multiple loci in a genome. These changes may include deletions, duplications, or amplifications at any locus as long as that region is represented on the array. Thus, array CGH is a coordinated and concurrent FISH experiment over hundreds or thousands of loci. In contrast, FISH on metaphase or interphase cells is limited by the number of probes that can be used simultaneously. In addition, FISH requires clinical suspicion that a specific locus in the genome has undergone copy-number change. This knowledge dictates the choice of probe for the FISH analysis and the examination of either interphase nuclei or metaphase chromosomes. Finally, FISH analysis on metaphase chromosomes detects only microdeletions, since FISH even on interphase nuclei may fail to identify duplications.

3.2 Principles and research applications of Array CGH

Array CGH is based on the same principle as traditional metaphase CGH. In both techniques, whole genomic DNA from a control (or reference) and genomic DNA from a test (or patient) are differentially labeled with two different fluorophores and used as probes that are cohybridized competitively onto nucleic acid targets. In traditional metaphase CGH, the target is a reference metaphase spread. In array CGH, these targets can be oligonucleotides, cDNAs, or genomic

fragments that are cloned in a variety of vectors such as plasmids, cosmids, BACs, or P1 artificial chromosomes.

The resolution of array CGH is defined by two main factors: 1) the size of the nucleic acid targets and 2) the density of coverage over the genome; the smaller the size of the nucleic acid targets and the more contiguous the targets on the native chromosome, the higher the resolution of the array. The use of array CGH in research has accelerated the pace of gene discovery in human genetics, deepened the understanding of genomic changes in cancer, and furthered the study of fundamental concepts related to chromosome conformation, DNA methylation, histone acetylation, gene silencing, replication timing, and many other basic mechanisms pertaining to DNA structure and function[36,37]. The high resolution afforded by array CGH has been used to define candidate regions for putative genes responsible or human genetic diseases. For example, Vissers et al[38] hybridized cell lines from two individuals with CHARGE syndrome onto a genome-wide array with a 1-Mb resolution. The authors used a 918-BAC tiling resolution array to narrow a candidate region for CHARGE syndrome on 8q12 based on data from two individuals, one with a 5-Mb deletion and another with a more complex rearrangement comprising two deletions that overlapped that of the first deletion subject. These results allowed the authors to focus on only nine genes in the region and detect heterozygous mutations in the gene CHD7, which was eventually shown to be the gene for CHARGE syndrome. The high resolution of that array was crucial in refining the critical region for this diseaseand in reducing the number of candidate genes to be investigated further. Array CGH has proven useful in providing DNA copy number “signatures” or profiles for various cancers. Many cancers are associated with multiple gains and losses of chromosomes and chromosomal segments. Given the difficulties associated with culturing and obtaining quality metaphases from most solid tumors, approaches that directly examine the DNA content and link any dosage changes to chromosome abnormalities are highly desired.

The hope of these studies is that certain signatures become prognostic markers and can guide

clinical treatments. Array CGH has been applied to a large number of cancer studies with reproducible results[35].

3.3 a-CGH and olfactory neuroblastoma

The cytogenic data on ONB from the literature are rather sparse: therefore we decided to compare our results with those Guled et al. (2008), who reported a-CGH results obtained on 13 patients, and reviewed all previous reports in the literature. Early suggestions that ONB is a form of peripheral neuroectodermal tumour have been subsequently disproven in multiple studies. In these studies, reverse transcriptase-PCR or FISH failed to find the EWS-FLI1 fusion transcript or EWS rearrangement in any candidate ONB. These findings explain the demonstrated absence of CD99 immunohistochemical staining in ONB[39].

In 1997 Szymas et al describe genomic imbalances of olfactory neuroblastoma in a 46-year-old woman by using the molecular cytogenetic technique - comparative genomic hybridization (CGH) for the first time in order to define the spectrum of genetic abnormalities in the tumor.

The CGH analysis showed multiple changes including DNA overrepresentations of chromosomes 4, 8, 11 and 14, partial DNA gains of the long arms of chromosomes 1 and 17, deletions of the entire chromosomes 16, 18, 19 and X, and partial losses of chromosomes 5q and 17p. This study represents an early utilisation of the CGH technique in olfactory neuroblastoma and demonstrates that the tumour carries complex chromosomal aberrations[40].

In the study of Riazimand the genomic imbalances of three ONB were analyzed by CGH to evaluate a recurrent pattern of imbalances and its relation to the pPNET family. The CGH analysis revealed multiple recurrent aberrations including DNA overrepresentations of chromosomal material of the entire chromosome 19, partial gains of the long arms of chromosomes 8, 15, and 22, and deletions of the entire long arm of chromosome 4. Beside these common aberrations, several single gains and losses occurred, that is, gains on 6p, 10q, 1p, 9q, and 13q. Their findings confirmed the former observation of amplified genetic material on chromosome 8 and found several new, currently not described recurrent genetic aberrations distinct from those described for pPNET and

give evidence that ONB is not part of the pPNET family. They suggest that the combined gain of genetic material on 15q, 22q, and chromosome 8 might be indicative for ONB [41].

Bockmuhl et al. reported on findings in ONB by conventional comparative genomic hybridization including frequent deletions of 1p, 3p/q, 9p, and 10p/q, and amplifications of 17q, 17p13, 20p, and 22q. They also noted a deletion on chromosome 11 and gain on chromosome 1p, which were apparently associated with metastasis and a worse prognosis. The study included 12 patients[42].

Table 8: Most common alterations in ONB found in Bockmuhl's paper

	DNA losses	DNA gains
Frequency of alterations		
90-100%	3p12-p14	17q12, 17q25
>80%	1p21-31, 3p/q, 9p, 10p/q	17p13, 20q, 22q11.2, 22q13
>70%	12q21,	7q11.2, 11q13, 14q32.2, 16p11.2, 16p13.3, 17q21-q24, 20p
>50%	1q24-q32, 2q22-q32, 4p/q, 5p14, 5q, 6q14-q23, 9q22-q33, 12p11.2-p12, 13q, 18q, 21q21	1q12, 14q, 16q, 19p/q
Pronounced deletions	4p13-p15, 10q26, 13q21-q23	
Pronounced gains		1p34, 1q23-q31, 7p21, 7q31, 9p23-p24, 17q11-q22, 17q24-q25, 19, 20p, 20q13, 22q13
Alterations associated with		
worse prognosis	4p/q, 5p/q, 6q, 7q31-q32, 9p, 11p/q,15q21	1q12, 8q, 20q
metastasis formation	5p/q, 6q, 7q31-q32, 11p12-p14, 11q14-q22, 15q21	1p32-p34, 1q12, 2p22-p24

Another study by Holland et al. has similarly shown complex cytogenetic changes in ONB. They performed comprehensive cytogenetic analyses of an ONB, Hyam's grade III-IV, using trypsin-Giemsa staining (GTG banding), multicolor fluorescence in situ hybridization (M-FISH), and locus-specific FISH complemented by molecular karyotyping using high-density single nucleotide polymorphism arrays. Therefore, their study supported the usefulness of applying complementary methods for cytogenetic analysis[43] (Table 9).

Structural aberations found in 25 metaphases using GTC banding

Chromosome no.	Structural chromosomal aberrations
1	**del(1)(p12p21)[2/25], del(1)(p22p32)[2/25], del(1)(p31p33)[2/25],** dup(1)(q25q32), dup(1)(q25q41)
2	del(2)(q31q33), **del(2)(q37)[4/25]**
3	**del(3)(p11p13)[6/25],** del(3)(p12p14), **del(3)(p25)[3/25],** del(3)(q25), del(3)(q26)
6	del(6)(p21), **del(6)(q12q14)[2/25], del(6)(q22q24)[3/25]**
10	del(10)(q26)
11	del(11)(q23)
15	del(15)(q26)
16	dup(16)(p13.3), dup(16)(q13q22)
17	dup(17)(p12), dup(17)(p13), i(17)(q10), **dup(17)(q25)[2/25]**
20	del(20)(q11.1q12)
21	**del(21)(q22)[3/25]**
22	**del(22)q(13)[5/25]**

Table 9: cytogenetic features showed in Holland's paper

Guled et al. performed an oligonucleotide-based aCGH analysis on 13 olfactory neuroblastoma samples, which was the first time that array-based CGH was applied to study the copy number changes in this neoplasm. Several copy number changes reported in previous studies were observed in their study, with identical, overlapping, or slightly different minimal common regions of alteration. Gains at the distal parts of 1p, 4, 9p, 13q, 15q, 22q, and 21q, and deletions at 4p and X, were reported in at least one study. Gains at 7q11 and 20q and deletions at 2q, 5q, 6p, 6q, and 18q were detected in two studies.

Overall, olfactory neuroblastomas have highly complex copy number changes that occur over the entire genome. All samples analyzed showed genomic imbalances with slightly more gains than losses. a-CGH revealed more copy number changes than previous studies that used conventional CGH. Furthermore, their results showed novel aberrations, which were not described in previous reports. In accordance with at least two previous studies, they found gains at 7q11.2 and 20q13, and

losses at 2q31–q37, 5q, 6p, 6q, and 18q. In addition to these previously reported alterations, they identified novel gains in their samples at 5q34–q35, 6p12.3, 10p12.31, 12q23.1–q24.31, and all of chromosome X. Losses at 15q11.2–q24.1, 15q13.1, 19q12–q13, 22q11.1–q11.21, 22q11.23, and 22q12.1 have not been described previously.

They identified a 770 kb region of chromosomal gain at 7q11.2. This region has been implicated in other cancers, and is overexpressed in prostate carcinomas, adenoid cystic carcinomas, head and neck squamous cell carcinomas, and pancreatic endocrine tumors.

A 6 Mb region of gain at 20q13.32–q13.33 was also identified. DNA copy number increases at chromosome 20q13 have been observed frequently in a variety of cancers, including breast, ovarian, and squamous cell carcinomas, suggesting that the region harbors one or more oncogenes.

Losses occurring at chromosome 2q have been described for various carcinomas, including head and neck squamous cell carcinoma, breast carcinoma, lung carcinoma, neuroblastoma, cervical cancer and prostate adenocarcinoma. Studies using different approaches have increasingly shown that the most affected region is 2q32–q37. This region also seems to be implicated in the development of ONB, as it has been reported in three cytogenetic studies including their investigation.

Another area of loss identified in their study, and also reported by Bockmuhl et al. and Holland et al., is located at 6q21–22. This region is frequently deleted in a variety of neoplasms, including pancreatic endocrine tumours, prostate carcinoma, breast carcinoma, and central nervous system lymphomas.

Their study also identified two small gains at 9p13.3 (782 kb) and 13q34 (363 kb) that were previously reported by Holland et al. The 9p13.3 locus has been shown to be gained in prostate cancer cell lines in two recent studies using aCGH. Gains at 13q34 have also been described previously in different cancers, including breast cancer, hepatocellular carcinoma, esophageal squamous cell carcinoma, and lung adenocarcinoma.

As for most tumors, stage is the most important parameter associated with survival in olfactory neuroblastoma. Their results clearly indicate that alterations in 20q and 13q are important in the progression of olfactory neuroblastoma. Gain of 20q has been widely associated with progression of several tumours, including breast carcinoma, cervical carcinoma, and pancreatic carcinoma. Both losses and gains of chromosome 13q have been noted in many recent studies of various tumours, suggesting the existence of novel oncogenes or tumour suppressor genes or both in this region. Furthermore, this region has been reported to contain microRNAs that could function as tumour suppressor genes or oncogenes[7].

Gains of both 13q and 20q are seen in colorectal carcinomas and their progression.

A number of genes located at these sites have been suggested to be important, but none of these changes has been sufficiently recurrent overall to be helpful in diagnosis, prognosis, or treatment and there have been no single gene mutations found in ONB to unify the entity or aid in its diagnosis. These various studies have, however, identified candidate regions for further study[44] .

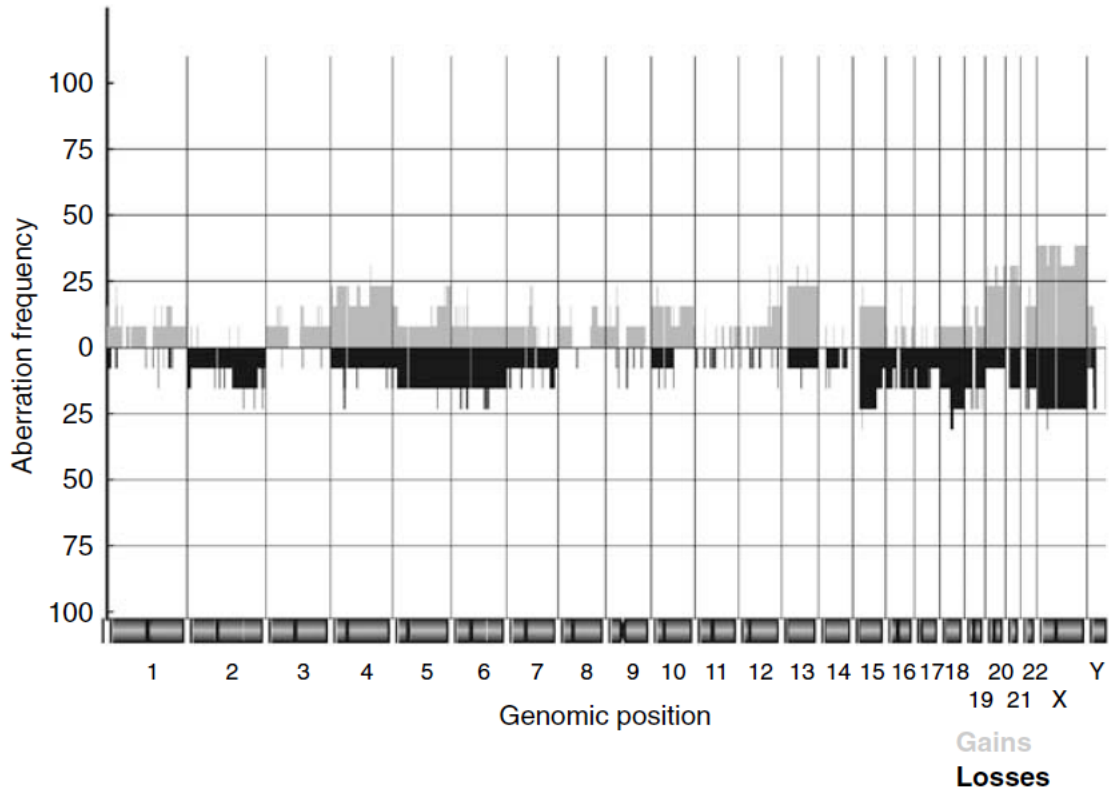

Fig. 4 Frequency profile of copy number aberrations in 13 olfactory neuroblastoma samples. CGH Explorer software and Piecewise

Constant Fit algorithm were used to determine copy number aberrations in olfactory neuroblastoma samples. The chromosomal alterations are shown in each probe position as incidence bar. Gains of genomic material are indicated in gray on the upper side of the middle line (at 0). Losses are indicated in black on the bottom side of the middle line. Genomic positions of the aCGH probes are marked on the x axis.

4. MATHERIALS AND METHODS

4.1 Patients

In our study we analyzed DNA from 13 patients affected by ONB and treated at the Ospedale di Circolo di Varese, University of Insubria.

The patients were diagnosed and staged using the Kadish system (Kadish et al., 1976), and Hyams' criteria (Hyams et al., 1988) were used for histological grading of the tumors. In each case, the diagnosis of ONB was established with hematoxylin/ eosin stained tissue sections and based on microscopic findings. In total, we a-CGH assayed 14 samples: ten primary tumors, two relapsed tumors, and two samples were from the same patient at onset and at relapse. DNA was extracted from paraffin-embedded tissues in nine cases, choosing the area in which the tumor cells represented > 50% of the total cell population, while four DNA samples were derived from fresh tumor material (Table 10).

Table 10 Clinical data on olfactory neuroblastomas

N.	Age	Sex	Kadish stage	Hyam's grade	P / R	Surgical treatment	F-up	Status	DNA
1	53	M	B	II	P	ERTC	179	AWD	DNA (FFPE)
					R				DNA (FFPE)
2	62	F	C	III	P	ERTC	113	NED	DNA (FFPE)
3	64	M	C	II	R	CER	126	AWD	DNA (FRESH)
4	41	M	B	II	R	CER	166	NED	DNA (FFPE)
5	69	M	C	II	P	ERTC	139	NED	DNA (FFPE)
6	33	F	B	II	P	ERTC	66	NED	DNA (FFPE)
7	77	F	B	I	P	ERTC	82	NED	DNA (FFPE)

8	33	F	B	II	P	ERTC	100	NED	DNA (FRESH)
9	44	M	C	II	P	ERTC	86	NED	DNA (FFPE)
10	48	M	B	II	P	ERTC	81	NED	DNA (FFPE)
11	80	F	B	III	P	ERTC	50	NED	DNA (FFPE)
12	62	F	C	II	P	ERTC	27	NED	DNA (FRESH)
13	53	F	C	II	P	ERTC	14	NED	DNA (FRESH)

P/R: primitive/relapse

ERTC: endoscopic resection with transnasal craniectomy; CER: cranioendoscopic resection

Follow-up in months

NED: no evidence of disease; AWD: alive with disease

FFPE: fixed and paraffin-embedded material; FRESH: tumor tissue obtained during surgery

Table 10 summarizes the surgical treatment, the disease status and the follow-up time for each patient, together with some clinicopathological data. Follow-up of the patients ranged from 14 to 179 months, with a mean of 60 months. Patient age ranged from 33 to 80 years, and all patients are alive. Two patients are alive with disease (leptomeningeal metastases). All patients received a radical surgical treatment and underwent postoperative radiotherapy except patient no.1 that refused it.

4.2 Hystological method

All tissues were fixed in buffered formalin (formaldehyde 4% w/v and acetate buffer 0.05M) and routinely processed to paraffin wax. Five µm-thick sections were stained with hematoxylin-eosin

(H&E) for morphological evaluation. For immunohistochemistry, three µm-thick sections were mounted on poly-L-lysine coated slides, deparaffinized and hydrated through graded alcohols to water. After endogenous peroxidase activity inhibition, performed by dipping sections in 3% hydrogen peroxide for 10 minutes, sections were treated in citrate buffer pH 6 in a microwave oven at 750W for 10 minutes for antigen retrieval. Successively, sections were incubated with primary antibodies at 4°C for 18–20 hours, followed by the avidin-biotin complex (ABC) procedure. Immunoreactions were developed using 0.03% 3,3'diaminobenzidine tetrahydrochloride and then sections were counterstained with Harris' hematoxylin. Specificity controls consisted of substitution of the primary antibody with non immune serum of the same species at the same dilution and use of control tissues with or without the pertinent antigen.

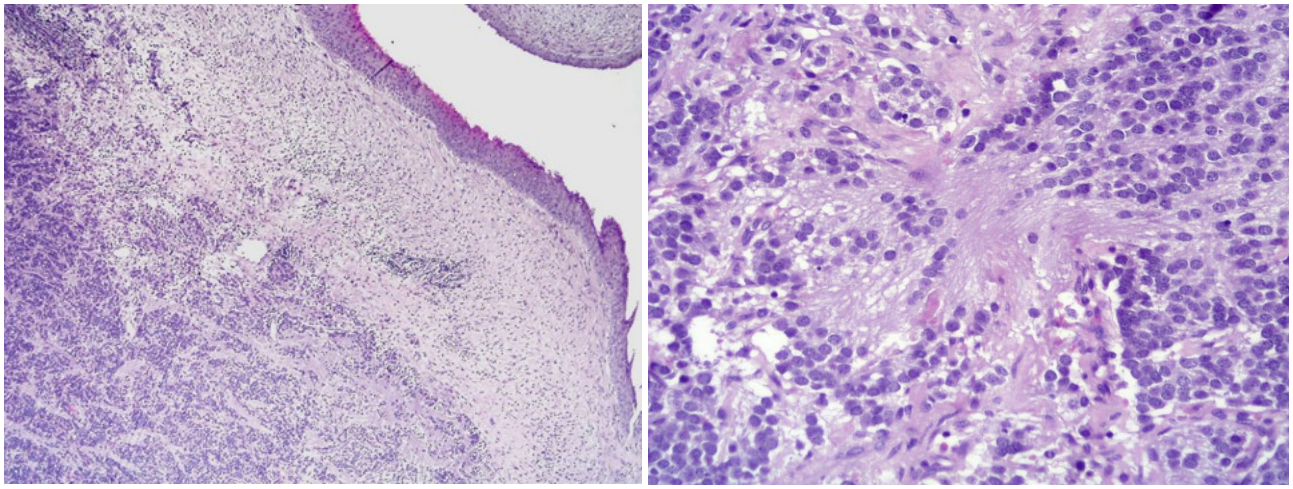

Figure 5: histological features of ONB

4.3 Technique of a-CGH

At the Department of Clinical and Experimental Medicine, University of Insubria of Varese, was performed the genetic analysis for identification and characterization of DNA imbalances in olfactory neuroblastomas by oligonucleotide array-based CGH.

DNA was obtained from nine formalin-fixed and paraffin-embedded tissue samples using representative 8-mm sections of the tumor samples. In detail, three sections from each specimen were treated twice with xylene, and then washed twice with ethanol. DNA was extracted using the QIAampVR DNA FFPE Tissue kit (Qiagen, Hilden, Germany) according to the manufacturer's protocol. Neoplastic areas were manually microdissected for DNA extraction and contained at least 50% tumor cells, to minimize contamination by normal cells[45]. For fresh specimens the average percentage of tumor cells was first evaluated during surgery by frozen section examination.

Sections of these specimens with >50% tumor cells were then mechanically reduced into tiny pieces, and DNA was then extracted with the Quiagen Blood and Tissue kit (QIAGEN GmbH, Hilden, Germany). Chromosome imbalances were defined by a-CGH with the whole-genome 244K platform (Agilent Technologies, Santa Clara, CA) according to the manufacturer's instructions for samples 1 and 5, while in samples nos. 2-4, 6-13 a 4x180K platform was used. The Agilent reference protocol used was: "Agilent Oligonucleotide Array-Based CGH for Genomic DNA Analysis Enzymatic Labelling for Blood, Cells or Tissues (version 7.1)." Slide images were acquired with Agilent's microarray scanner G2565CA and features were extracted by Agilent's Feature Extraction 10.7.3.1 software, and the a-CGH profiles were extrapolated with the Agilent's Genomic Workbench software 6.5.0.18 using the following parameters/algorithms: ADM2 (Threshold 6.0), Fuzzy zero (on), Centralization (on), default feature filter (on). An aberration filter algorithm (parameters: minimum number of probes per region =15, minimum absolute average log ratio values per region =0.3, maximum number of aberrant region =100, percent of penetrance per features =0) was applied to filter-out all the aberrations below 30% of mosaic level [46].

The Agilent Oligonucleotide Array-Based CGH for Genomic DNA Analysis (for FFPE Samples) user guide (Version 1.0, P/N G4410-90020) is available at www.agilent.com/chem/dnamanuals-protocols for a detailed description of the protocol used.

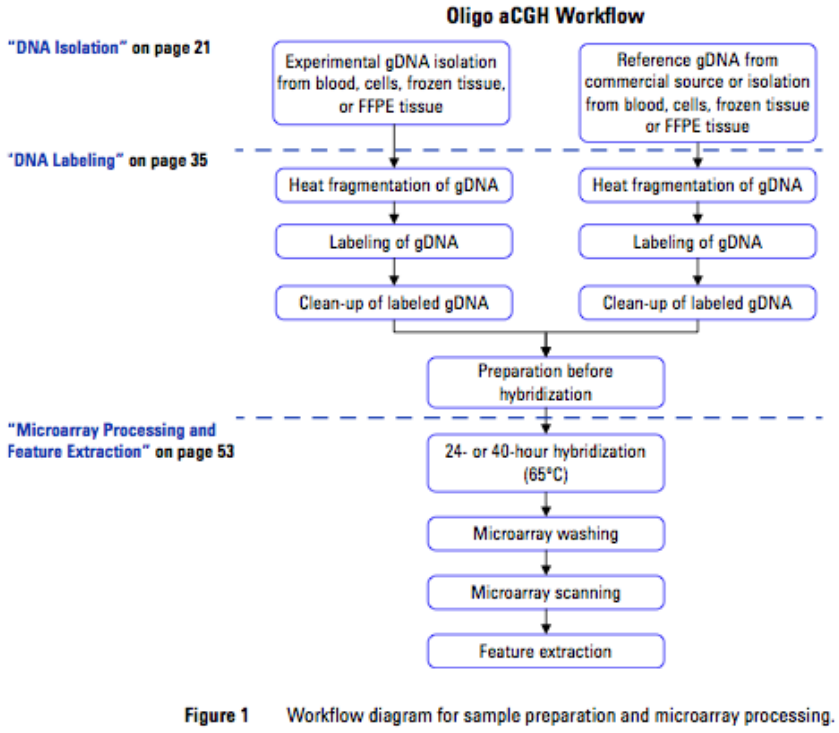

Figure 1 Workflow diagram for sample preparation and microarray processing.

Figure 6: a-CGH workflow diagram for sample preparation and microarray processing

Purification of genomic DNA from formalin-fixed, paraffin-embedded tissues (FFPE)

The procedure to isolate genomic DNA (gDNA) from formalin-fixed paraffin-embedded (FFPE) samples is based on the method described by van Beers et al. (van Beers et al 2006) using the

Qiagen DNeasy Blood & Tissue Kit (p/n 69504).

The protocol used is from QIAGEN Technical Service Departments (www.qiagen.com)

Procedure:

Step 1. Paraffin Removal

1. Equilibrate a heat block or water bath to 90 °C and a thermomixer to 37 °C.

2 .Put up to 5 20-micron FFPE sections into a 1.5 mL nuclease-free microfuge tube.

3. Prepare 10% Tween 20, by adding 100 µL Tween 20 to 900 µL of nuclease-free water. The solution can be prepared in advance and stored up to 6 months at room temperature.

4. Add 480 µL PBS and 20 µL 10% Tween 20 to the FFPE sections in the 1.5 mL nuclease-free microfuge tube.

5. Transfer the sample tube to a circulating water bath or heat block at 90 °C. Incubate at 90 °C for 10 minutes.

6. Spin immediately for 15 minutes at 10,000 x g in a microcentrifuge. Put the sample tube on ice for 2 minutes.

7. Remove the resulting wax disc with a pipette tip or tweezers. Remove and discard the supernatant without disturbing the pellet.

8. Add 1 mL of 100% ethanol to the pellet and vortex briefly. Spin for 5 minutes at 10,000 x g in a microcentrifuge.

9. Remove ethanol without disturbing the pellet and let the sample tube sit at room temperature with the lid open until residual ethanol has completely evaporated.

10. Prepare a 1M NaSCN solution by adding 10 g of NaSCN to 123 mL of nuclease free water. The solution can be prepared in advance and stored up to 1 month at room temperature.

11. Add 400 µL 1M NaSCN to the dry pellet and briefly mix on a vortex mixer.

12. Transfer the sample tube to a thermomixer at 37 °C. Incubate overnight at 37 °C. Shake at 450 rpm.

Step 2. Proteinase K Treatment

1. Equilibrate a thermomixer to 55 °C.

2. Transfer the sample tube to a microcentrifuge. Spin for 20 minutes at 10,000 x g.

3. Remove and discard the supernatant without disturbing the pellet.

4. Add 400 µL PBS to the pellet and vortex briefly.

5. Spin again for 20 minutes at 10,000 x g in a microcentrifuge.

6. Remove and discard the supernatant without disturbing the pellet.

7. Add 360 µL of Qiagen buffer ATL (supplied with Qiagen DNeasy Blood & Tissue Kit).

8. Add 40 µL proteinase K (supplied), mix well on a vortex mixer, and incubate overnight in a thermomixer at 55 °C shaking at 450 rpm.

9. Transfer the sample tube to a microcentrifuge. Spin for 30 seconds at 6,000 x g to drive the contents off the walls and lid.

10. Add 40 µL proteinase K, mix well on a vortex mixer, and incubate in a thermomixer for approximately 6 to 8 hours at 55 °C shaking at 450 rpm.

11. At the end of the day, transfer the sample tube to a microcentrifuge and spin for 30 seconds at 6,000 x g to drive the contents off the walls and lid.

12. Add 40 µL proteinase K, mix well on a vortex mixer and incubate overnight in a thermomixer at 55 °C shaking at 450 rpm.

Step 3. gDNA Extraction

1. Equilibrate a heat block or water bath to 56 °C.

2. Let samples cool to room temperature and spin in a microcentrifuge for 30 seconds at 6,000 x g to drive the contents off the walls and lid.

3. Add 8 µL of RNase A (100 mg/mL), mix on a vortex mixer, and incubate for 2 minutes at room temperature. Transfer the sample tube to a microcentrifuge and spin for 30 seconds at 6,000 x g to

drive the contents off the walls and lid.

4. Add 400 µL Buffer AL (supplied), mix thoroughly on a vortex mixer, and incubate in a circulating water bath or heat block at 56 °C for 10 minutes. Transfer the sample tube to a microcentrifuge and spin for 30 seconds at 6,000 x g to drive the contents off the walls and lid.

5. Add 440 µL 100% ethanol, and mix thoroughly on a vortex mixer. Transfer the sample tube to a microcentrifuge and spin for 30 seconds at 6,000 x g to drive the contents off the walls and lid.

6. Put two DNeasy Mini spin columns in two clean 2 mL collection tubes (supplied). Split the entire sample mixture onto two DNeasy Mini spin columns (i.e. 660 µL each).

7. Spin in a microcentrifuge for 1 minute at 6,000 x g. Discard the flow-through and collection tube. Put the DNeasy Mini spin columns in fresh 2 mL collection tubes (supplied).

8. Before using for the first time, prepare Buffer AW1 by adding 100% ethanol to the Buffer AW1 bottle (supplied; see bottle label for volume). Mark the appropriate check box to indicate that ethanol was added to the bottle.

9. Add 500 µL Buffer AW1 onto each spin column, and spin in a centrifuge for 1 minute at 6,000 x g. Discard the flow-through and collection tube. Put the DNeasy Mini spin columns in fresh 2 mL collection tubes (supplied).

10. Prepare a fresh 80% ethanol solution by adding 40 mL 100% ethanol to 10 mL nuclease-free water.

11. Add 500 µL 80% ethanol onto each column, and spin in a microcentrifuge for 3 minutes at 20,000 x g to dry the column membrane. Discard the flow-through and collection tube.

12. Put the DNeasy Mini spin column in a clean 1.5 mL microcentrifuge tube, and add 50 µL of nuclease free water directly to the center of each spin column.

13. Let stand at room temperature for 1 minute, and then spin in a microcentrifuge for 1 minute at 6,000 x g to elute the DNA.

14. Combine the purified DNA from the same sample in one microcentrifuge tube for a final total

volume of 100 µL.

DNA Labeling

Step 1. Preparation of gDNA Before Labeling

1. Estimate the average molecular weight for each gDNA sample based on the agarose gel analysis

2. If the gDNA concentration isless than required, concentrate the sample using a concentrator before you continue to the heat fragmentation.

3. Put the appropriate amount of gDNA and nuclease-free water in a 0.2 mL nuclease-free PCR tube or plate to achieve the volumes

Step 2. Heat Fragmentation

1. Incubate the gDNA at 95 °C in a thermocycler with heated lid for the time to fragment the gDNA.

2. Transfer the sample tubes to ice and incubate on ice for 3 minutes. You can also hold at 4 °C for 3 minutes in a thermocycler.

3. Spin in a microcentrifuge for 30 seconds at 6,000 × g to drive the contents off the walls and lid.

Step 3. ULS Labeling

1.Prepare one Cy3 and one Cy5 Labeling Master Mix by mixing the components, based on your microarray format and sample type. Avoid pipetting volumes less than 2 µL to ensure accuracy.

2.Add the appropriate amount of Labeling Master Mix to each PCR tube containing the gDNA to make a total volume. Mix well by gently pipetting up and down.

3.Transfer PCR tubes or plates to a thermocycler with heated lid and incubate at 85 °C for 30 minutes.

4.Transfer the samples to ice and incubate on ice for 3 minutes. You can also hold at 4 °C for 3 minutes in a thermocycler.

5.Spin in a microcentrifuge for 1 minute at 6,000 × g to drive the contents off the walls and lid.

Labeled gDNA can be stored on ice until dye removal using the Agilent KREApure columns or the Agilent Genomic DNA 96-well Purification Module.

Step 4. Removal of non-reacted ULS-Cy

Non-reacted ULS-Cy3 or ULS-Cy5 can interfere with the subsequent microarray experiment and increase background noise if they are not efficiently removed prior to hybridization. The Agilent KREApure columns or Genomic DNA 96-well Purification Module effectively removes non-reacted ULS dye.

Preparation of Labeled Genomic DNA for Hybridization

1. Prepare the 100X Blocking Agent:

a. Add 135 µL of nuclease-free water to the vial containing lyophilized 10X CGH Blocking Agent (supplied with Agilent Oligo aCGH Hybridization Kit).

b. Mix briefly on a vortex mixer and leave at room temperature for 60 minutes to reconstitute sample before use or storage.

c. Cross out "10X" on the label on the blocking agent vial and write "100X". You are actually making a 100X Blocking Agent, so you need to relabel the

vial of lyophilized blocking agent as such.

The 100X Blocking Agent can be prepared in advance and stored at -20 °C.

2. Equilibrate water baths or heat blocks to 95 °C and 37 °C or use a thermocycler.

3. Prepare the Hybridization Master Mix by mixing the components in the table below according to the microarray format.

4. Add the appropriate volume of the Hybridization Master Mix to the 1.5 mL microfuge tube, tall chimney plate well or PCR plate well containing the labeled gDNA to make the total volume

5. Mix the sample by pipetting up and down, and then quickly spin in a centrifuge to drive the contents off the walls and lid.

6. Incubate the samples:

a Transfer sample tubes to a circulating water bath or heat block at 95 °C.

Incubate at 95 °C for 3 minutes.

b Immediately transfer sample tubes to a circulating water bath or heat block at 37 °C. Incubate at 37 °C for 30 minutes or Transfer sample tubes to a thermocycler. Program the thermocycler

7. Remove sample tubes from the water bath, heat block or thermocycler. Quickly spin in a centrifuge to drive the contents off the walls and lid.

8. Bring the Agilent-CGHblock (supplied with the ULS Labeling Kit) to room temperature.

Make sure that the Agilent-CGHblock is completely equilibrated to room temperature before you continue.

9. Add the appropriate volume of Agilent-CGHBlock to each well or 1.5 mL microfuge tube containing the labeled gDNA and Hybridization Master Mix to make the final volume of hybridization sample mixture.

Mix well by pipetting up and down.

10. Quickly spin in a centrifuge to drive the contents off the walls and lid.

Microarray Processing and Feature Extraction

Step 1. Microarray Hybridization

Step 2. Wash Preparation

Step 3. Microarray Washing

Step 4. Microarray Scanning using Agilent SureScan, C or B Scanner

Step 5. Data Extraction using Feature Extraction Software

Microarray processing consists of hybridization, washing, and scanning.

Feature Extraction is the process by which data is extracted from the scanned microarray and translated into log ratios, allowing researchers to measure DNA copy number changes in their experiments in conjunction with Agilent Genomic Workbench Software.

Step 1. Microarray Hybridization

Hybridization Assembly

1. Load a clean gasket slide into the Agilent SureHyb chamber base with the gasket label facing up and aligned with the rectangular section of the chamber base. Ensure that the gasket slide is flush with the chamber base and is not ajar.

2. Slowly dispense 490 µL (for 1x microarray), 245 µL (for 2x microarray), 100 µL (for 4x microarray) or 40 µL (for 8x microarray) of hybridization sample mixture onto the gasket well in a "drag and dispense" manner. For multi-pack microarray formats (i.e. 2x, 4x or 8x microarray), load all gasket wells before you load the microarray slide. For multi-pack formats, refer to "Agilent Microarray Layout and Orientation"

3. Put a microarray slide "active side" down onto the gasket slide, so the numeric barcode side is facing up and the "Agilent"-labeled barcode is facing down. Assess that the sandwich-pair is properly aligned.

4. Put the SureHyb chamber cover onto the sandwiched slides and slide the clamp assembly onto both pieces.

5. Hand-tighten the clamp firmly onto the chamber.

6. Vertically rotate the assembled chamber to wet the slides and assess the mobility of the bubbles. Tap the assembly on a hard surface if necessary to move stationary bubbles.

7. Put assembled slide chamber in the rotator rack in a hybridization oven set to 65 °C. Set your hybridization rotator to rotate at 20 rpm.

8. Hybridize at 65 °C: • 24 hours for blood, cell and tissue samples (4x and 8x microarrays) • 40 hours for blood, cell and tissue samples (1x and 2x microarrays) • 40 hours for FFPE samples (1x, 2x, 4x and 8x microarray)

Step 2. Wash Preparation

Cleaning with Milli-Q Water Wash

Rinse slide-staining dishes, slide racks and stir bars thoroughly with high-quality Milli-Q water before use and in between washing groups.

a Run copious amounts of Milli-Q water through the slide-staining dishes, slide racks and stir bars.

b Empty out the water collected in the dishes at least five times. c Repeat step a and step b until all traces of contaminating material are removed.

Cleaning with Acetonitrile Wash

Acetonitrile wash removes any remaining residue of Agilent Stabilization and Drying Solution from slide-staining dishes.

a Add the slide rack and stir bar to the slide-staining dish, and transfer to a magnetic stir plate.

b Fill the slide-staining dish with 100% acetonitrile.

c Turn on the magnetic stir plate and adjust the speed

d Wash for 5 minutes at room temperature.

e Discard the acetonitrile as is appropriate for your site.

f Repeat step a through step e.

g Air dry everything in the vented fume hood.

h Continue with the Milli-Q water wash as previously instructed.

Prewarming Oligo aCGH Wash Buffer 2 (Overnight)

The temperature of Oligo aCGH Wash Buffer 2 must be at 37 °C for optimal performance.

1 Add the volume of buffer required to a disposable plastic bottle and warm overnight in an incubator or circulating water bath set to 37 °C.

2 Put a slide-staining dish into a 1.5 L glass dish three-fourths filled with milli-Q water and warm to 37 °C by storing overnight in an incubator set to 37 °C.

Prewarming Stabilization and Drying Solution (Wash Procedure B Only)

The Agilent Stabilization and Drying Solution contains an ozone scavenging compound dissolved in acetonitrile. The compound in solution is present in saturating amounts and may precipitate from the solution under normal storage conditions. If the solution shows visible precipitation, warming of the solution will be necessary to redissolve the compound. Washing slides using Stabilization and Drying Solution showing visible precipitation will have profound adverse affects on array performance.

1 Put a clean magnetic stir bar into the Stabilization and Drying Solution bottle and recap.

2 Partially fill a plastic bucket with hot water at approximately 40 °C to 45 °C (for example from a hot water tap).

3 Put the Stabilization and Drying Solution bottle into the hot water in the plastic bucket.

4 Put the plastic bucket on a magnetic stirrer (not a hot-plate) and stir.

5 The hot water cools to room temperature. If the precipitate has not all

dissolved replenish the cold water with hot water.

6 Repeat step 5 until the solution is clear.

7 After the precipitate is completely dissolved, allow the solution to equilibrate to room temperature prior to use.

Step 3. Microarray Washing

Wash Procedure A (without Stabilization and Drying Solution)

1 Completely fill slide-staining dish #1 with Oligo aCGH Wash Buffer 1 at room temperature.

2 Put a slide rack into slide-staining dish #2. Add a magnetic stir bar. Fill slide-staining dish #2 with enough Oligo aCGH Wash Buffer 1 at room temperature to cover the slide rack. Put this dish on a magnetic stir plate.

3 Put the prewarmed 1.5 L glass dish filled with water and containing slide-staining dish #3 on a magnetic stir plate with heating element. Fill the slide-staining dish #3 approximately three-fourths full with Oligo aCGH Wash Buffer 2 (warmed to 37 °C). Add a magnetic stir bar. Turn on the heating element and maintain temperature of Oligo aCGH Wash Buffer 2 at 37 °C; monitor using a thermometer.

4 Remove one hybridization chamber from incubator and resume rotation of the others. Record whether bubbles formed during hybridization and if all bubbles are rotating freely.

5 Prepare the hybridization chamber disassembly. a Put the hybridization chamber assembly on a flat surface and loosen the

thumbscrew, turning counter-clockwise.

b Slide off the clamp assembly and remove the chamber cover.

c With gloved fingers, remove the array-gasket sandwich from the chamber base by lifting one end and then grasping in the middle of the long sides. Keep the microarray slide numeric barcode facing up as you quickly transfer the sandwich to slide-staining dish #1.

d Without letting go of the slides, submerge the array-gasket sandwich into slide-staining dish #1 containing Oligo aCGH Wash Buffer 1.

6 With the sandwich completely submerged in Oligo aCGH Wash Buffer 1, pry the sandwich open from the barcode end only. Do this by slipping one of the blunt ends of the forceps between the slides and then gently twist the forceps to separate the slides. Let the gasket slide drop to the bottom

of the staining dish. Remove the microarray slide, grasp it from the upper corners with thumb and forefinger, and quickly put into slide rack in the slide-staining dish #2 containing Oligo aCGH Wash Buffer 1 at room temperature. Minimize exposure of the slide to air. Touch only the barcode portion of the microarray slide or its edges!

7 Repeat step 4 through step 6 for up to four additional slides in the group. A maximum of five disassembly procedures yielding five microarray slides is advised at one time in order to facilitate uniform washing.

8 When all slides in the group are put into the slide rack in slide-staining dish #2, stir using setting 4 for 5 minutes. Adjust the setting to get good but not vigorous mixing.

9 Transfer slide rack to slide-staining dish #3 containing Oligo aCGH Wash Buffer 2 at 37 °C, and stir using setting 4 for 1 minute.

10 Slowly remove the slide rack trying to minimize droplets on the slides. It should take 5 to 10 seconds to remove the slide rack.

11 Discard used Oligo aCGH Wash Buffer 1 and Oligo aCGH Wash Buffer 2.

12 Repeat step 1 through step 11 for the next group of five slides using fresh Oligo aCGH Wash Buffer 1 and Oligo aCGH Wash Buffer 2 pre-warmed to 37 °C.

13 Put the slides in a slide holder.

Figure 7: Slide in slide holder for SureScan microarray scanner

Wash Procedure B (with Stabilization and Drying Solution)

Cy5 is susceptible to degradation by ozone. Use this wash procedure if the ozone level exceeds 10 ppb in your laboratory.

Always use fresh Oligo aCGH Wash Buffer 1 and Oligo aCGH Wash Buffer 2 for each wash group (up to five slides).

The acetonitrile (dish #4) and Stabilization and Drying Solution (dish #5) below may be reused for washing up to 4 batches of 5 slides (total 20 slides) in one experiment. Do not pour the Stabilization and Drying Solution back in the bottle.

1 Completely fill slide-staining dish #1 with Oligo aCGH Wash Buffer 1 at room temperature.

2 Put a slide rack into slide-staining dish #2. Add a magnetic stir bar. Fill slide-staining dish #2 with enough Oligo aCGH Wash Buffer 1 at room temperature to cover the slide rack. Put this dish on a magnetic stir plate.

3 Put the prewarmed 1.5 L glass dish filled with water and containing slide-staining dish #3 on a magnetic stir plate with heating element. Fill the slide-staining dish #3 approximately three-fourths full with Oligo aCGH Wash Buffer 2 (warmed to 37 °C). Add a magnetic stir bar. Turn on the heating element and maintain temperature of Oligo aCGH Wash Buffer 2 at 37 °C; monitor using a thermometer.

4 In the fume hood, fill slide-staining dish #4 approximately three-fourths full with acetonitrile. Add a magnetic stir bar and put this dish on a magnetic stir plate.

5 In the fume hood, fill slide-staining dish #5 approximately three-fourths full with Stabilization and Drying Solution. Add a magnetic stir bar and put this dish on a magnetic stir plate.

6 Remove one hybridization chamber from incubator and resume rotation of the others. Record whether bubbles formed during hybridization, and if all bubbles are rotating freely.

7 Prepare the hybridization chamber disassembly.

a Put the hybridization chamber assembly on a flat surface and loosen the thumbscrew, turning counter-clockwise.

b Slide off the clamp assembly and remove the chamber cover.

c With gloved fingers, remove the array-gasket sandwich from the chamber base by lifting one end and then grasping in the middle of the long sides. Keep the microarray slide numeric barcode facing up as you quickly transfer the sandwich to slide-staining dish #1.

d Without letting go of the slides, submerge the array-gasket sandwich into slide-staining dish #1 containing Oligo aCGH Wash Buffer 1.

8 With the sandwich completely submerged in Oligo aCGH Wash Buffer 1, pry the sandwich open from the barcode end only. Do this by slipping one of the blunt ends of the forceps between the slides and then gently twist the forceps to separate the slides. Let the gasket slide drop to the bottom of the staining dish. Remove the microarray slide, grasp it from the upper corners with thumb and forefinger, and quickly put into slide rack in the slide-staining dish #2 containing Oligo aCGH Wash Buffer 1 at room temperature. Minimize exposure of the slide to air. Touch only the barcode portion of the microarray slide or its edges!

9 Repeat step 6 through step 8 for up to four additional slides in the group. A maximum of five disassembly procedures yielding five microarray slides is advised at one time in order to facilitate uniform washing.

10 When all slides in the group are placed into the slide rack in slide-staining dish #2, stir using setting 4 for 5 minutes. Adjust the setting to get good but not vigorous mixing.

11 Transfer slide rack to slide-staining dish #3 containing Oligo aCGH Wash Buffer 2 at 37 °C, and stir using setting 4 for 1 minute.

12 Remove the slide rack from Oligo aCGH Wash Buffer 2 and tilt the rack slightly to minimize wash buffer carry-over. Quickly transfer the slide rack to slide-staining dish #4 containing acetonitrile, and stir using setting 4 for 10 seconds.

13 Transfer slide rack to slide-staining dish #5 filled with Stabilization and Drying Solution, and stir using setting 4 for 30 seconds.

14 Slowly remove the slide rack trying to minimize droplets on the slides. It should take 5 to 10 seconds to remove the slide rack.

15 Discard used Oligo aCGH Wash Buffer 1 and Oligo aCGH Wash Buffer 2.

16 Repeat step 1 through step 15 for the next group of five slides using fresh Oligo aCGH Wash Buffer 1 and Oligo aCGH Wash Buffer 2 prewarmed to 37 °C.

17 Immediately put the slides with Agilent barcode facing up in a slide holder with an ozone-barrier slide cover on top of the array .

18 Scan slides immediately to minimize impact of environmental oxidants on signal intensities. If necessary, store slides in original slide boxes in a N2 purge box, in the dark.

19 Dispose of acetonitrile and Stabilization and Drying Solution as flammable solvents.

Step 4. Microarray Scanning using Agilent SureScan, C or B Scanner

Figure 8: agilent scanner

Step 5. Data Extraction using Feature Extraction Software

5. RESULTS

5.1 Clinical results

In our study we analyzed 14 samples of DNA from 13 patients affected by ONB and treated at the Ospedale di Circolo di Varese, University of Insubria

Gender and age. Patients are 6 male and 7 females and aged from 33 to 80 years old.

Presenting Symptoms. 13 patients complained of nasal obstruction either alone or associated with other symptoms; epistaxis in 8, mucous rhinorrhea in 6, headache in 3. One patient was asymptomatic and the diagnosis was incidental.

Site of Origin. All the tumors arose in the olfactory cleft.

Stage. According to the Kadish classification, the disease in 7 patients was classified as stage B and in 6 patients as stage C.

Hyams' Grading. Pathologic differentiation according to the Hyam's criteria revealed 1 patient Hyam's grade I, 10 patient Hyam's grade II and 2 patients Hyam's grade III. Grade I and II lesions are considered as low-grade tumors while grade III and IV lesions are considered as high-grade tumors.

Treatment. 11/13 patients underwent an endoscopic resection with trasnasal craniectomy (ERTC), 2 patients underwent a cranioendoscopic resection due to the intracranial involvement laterally to the virtual plane passing the lamina papyracea.

12/13 patients underwent an adjuvant RT on the primary site of tumour, one patient refused postoperative radiotherapy. In 1 patient RT was administered in association with systemic chemotherapy postoperatively, due to the periorbital extension and the young age. The mean dosage administered was 60 Gy.

Intraoperative Margins. In 12/13 of these cases, surgical margins were free of disease, in only one case with massive intracranial intradural involvement, extended laterally over the orbital roof,

infiltration of the margins was observed. This patient underwent an andoscopic endonasal resection becasuse the old age and the comorbidities contraindicated the external approach (cranioendoscopic approach).

Local, Regional and Distant Recurrence

2 patients presented a local recurrence of disease; none of the patients presented distant metastasis.

Survival. All the patients are alive: 2/13 alive with disease and 11/13 free of disease. Follow-up ranged from 14 to 179 months. Every patient regained his or her normal daily activities with excellent quality of life.

5.2 Hystopatological results

The olfactory neuroblastoma showed a low number of mitosis (counted in 10 fields at high magnification X400): on average 2 mitosis, with a variability between 0 and 6 mitoses; counts of MIB-1 (Ki-67) of 2000 neoplastic cells, showed a proliferative index of about 10%, with a range between 2% and 20%. In most cases, was not present angioinvasione and no tumour showed signs of neuroinvasione. In 7 patients bony structures invasion was present. Furthermore, only in 2 cases there were areas of necrosis.

In poorly differentiated neuroendocrine carcinomas mitotic counts for 10 HPF, was much higher (with an average value of 30 and with a variability of between 20 and 60 mitosis), the proliferative index MIB-1 (Ki-67, counted of 2000 cells) was equal to 46% with a variability between 20% and 80%.

In all cases it was evident the presence of necrosis, often with the characteristic appearance to "map". The angioinvasione, the neuroinvasione and infiltration of bone were present only in small part.

In olfactory neuroblastoma staining for synaptophysin was present in most cases, as the immunoreactivity for chromogranin A. It was also observed the expression of S-100 protein, and

not of cytokeratins.

While neuroendocrine carcinomas, cytokeratin AE1/AE3 was expressed in all carcinomas and there was no immunoreactivity for S100 protein.

5.3 a-CGH results

All a-CGH results are reported in Table 11 Chromosome gains are more common than losses and the most frequently affected chromosomes are 20 (in 9 samples out 14), 14 (9 samples out of 14), 19 (10 samples out of 14), 15 (8 samples out of 14), 17 (8 samples out of 14), 11,16, X (7 samples out of 14), 2 (6 samples out of 14), 13 (5 samples out of 14), 9 (2 samples out of 14), 21 (3 samples out 14), 10, 12 (1 sample out of 14). Only 2 samples show multiple losses of entire chromosomes. Frequent imbalances due to structural rearrangements are found in most chromosomes except 3,4,6,9,13,18 e X. Only one tumor do not display any imbalaces. In patient 1, in whom we tested both the primitive and relapsed tumor, no loss of an entire chromosome is observed in either samples. Notably, we observe an increased number of partial gains in the relapse, while the partial losses involve the same chromosome regions.

	1+	2+	3+	4+	5+	6+	7+	8+	9+	10+	11+	12+	13+	14+	15+	16+	17+	18+	19+	20+	21+	22+	X+	Y+
Pz.1-P		pq			pq	pq	pq		pq		pq		13q12-13q31.1		q	pq	pq	pq	pq	pq			pq	
PZ.1-R		p			pq	pq	pq				pq													
		q12-2q35																						
		2q36.1-2q36.3																						
Pz.2											pq			q	q			pq	p	pq				
Pz.3		2p12-2q12.1			pq		pq				pq		q	q	q	pq		pq	pq	pq	q	q	pq	
Pz. 4					5p13.3-p14.3	6p21.1-p22.2	7p22.1-pter				11p15.4-pter			14q32.11-qter		16p	pq	18q22.1	19p	20p13-pter	21q22.11-qter	pq		
							7q11.22-22.11				11p11.12-p11.2								9q	20q				
							7q22.1				11q12.2-q14.4													
											11q23.1-qter													
Pz. 5					pq	pq	pq				pq		13q	pq	pq	pq	pq	pq	pq	pq		pq	pq	pq
Pz. 6	1q32.1-q32.2	pq			pq	pq	pq				pq			pq	pq	pq	pq	pq	pq	pq		pq		
Pz. 7																								
Pz. 8					pq	pq	pq	8p12-p21.1	pq		q	p	p	p	p	pq	pq	pq		pq		q		
pz.9					pq	pq	pq				pq			q	q	pq	pq	pq	pq	pq		q	pq	pq
pz.10							7p21.3-pter		9p13.1-p13.3		11p15.4-pter									pq				
							7qcen-q21.11		9q33.2-qter		11q12.1-14.1													
							7q22.1-q22.2				11q22.3-qter													
pz.11		pq			pq	pq	pq			pq	pq	pq	q	q	q	pq	pq		pq	pq		q		
pz.12		pq			pq	pq	pq				11pter-q22.3		pq	pq		pq	pq		pq	pq	21q21.1-21.2	pq		
pz.13		pq			pq	pq	pq				pq			pq	pq	pq	pq		pq	pq	21q21.1-21.2	pq	pq	

Table 11: amplificated regions for patient and for chromosomes showed by the a-CGH

Table 12: loss regions for patients and for chromosomes showed by the a-CGH

	1-	2-	3-	4-	5-	6-	7-	8-	9-	10-	11-	12-	13-	14-	15-	16-	17-	18-	19-	20-	21-	22-	X-	Y-
1-P	p31.1-p12																							q
	q23.1-q25.1											q24.21												
1-R	p31.1-p12																							
	q23.1-q25.1																							q
2																								
3																								q
4	1 (complesso)		3 compl	pq				pq	9 compl	pq		12 compl	pq		pq						q21.1-q21.3		p11.4-21.3	
5	q31.1-q32.1		3pcen-p12.3					p23.1-p23.2																
			3q21-q26.2																					
6																								
7																								
8																								
9																								
10	pcenp33		pq	pq				pq		pq	11p11.2-p12	p												
	q23.1-qter											qcen-q13.11												
												q14.1-q24.11									q21.1-q22.11			pq
11																								
12	p32.3-13.2																	pter-q12.1					p21.1	
13																								

The most frequent alterations involved the amplification of chromosoma 5,7, 11 and 20, which are presented in 80% of the patients. Alterations occurring in at least 60% of the cases are amplification of whole chromosoma 16, 17, 19, amplification of short arm of chromosome (p) 6 and

amplification of long arm of chromosome (q) 14, 18 and 22.

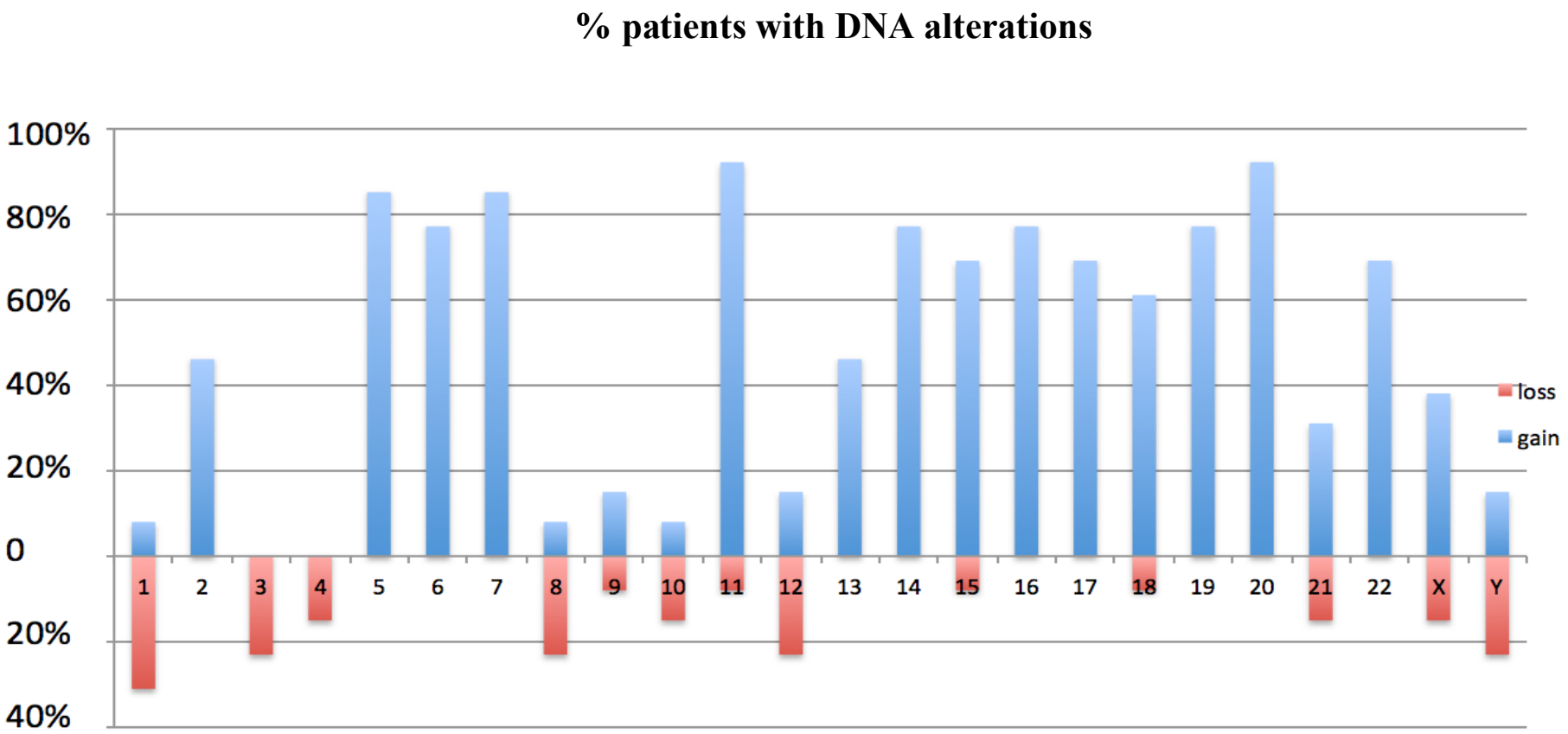

Figure13: percentage of patients with DNA gain or loss for each chromosome. The Y axis shows the percentage of patients with gain or loss in chromosome. The X axis indicates the chromosome number.

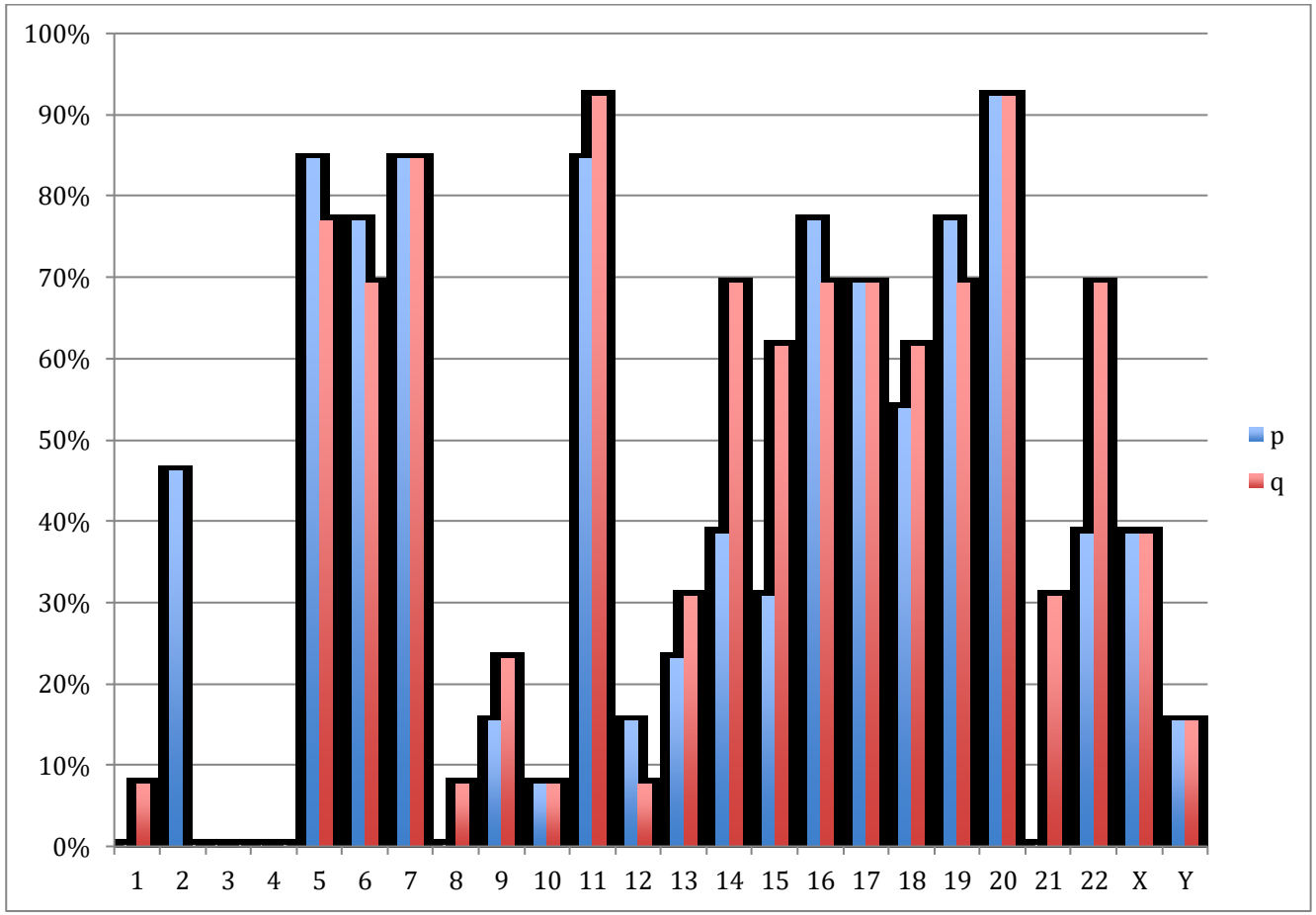

Figure 14: chromosomal gains. The Y axis shows the percentage of patients. The x axis shows the short and long arm gains for each chromosome.

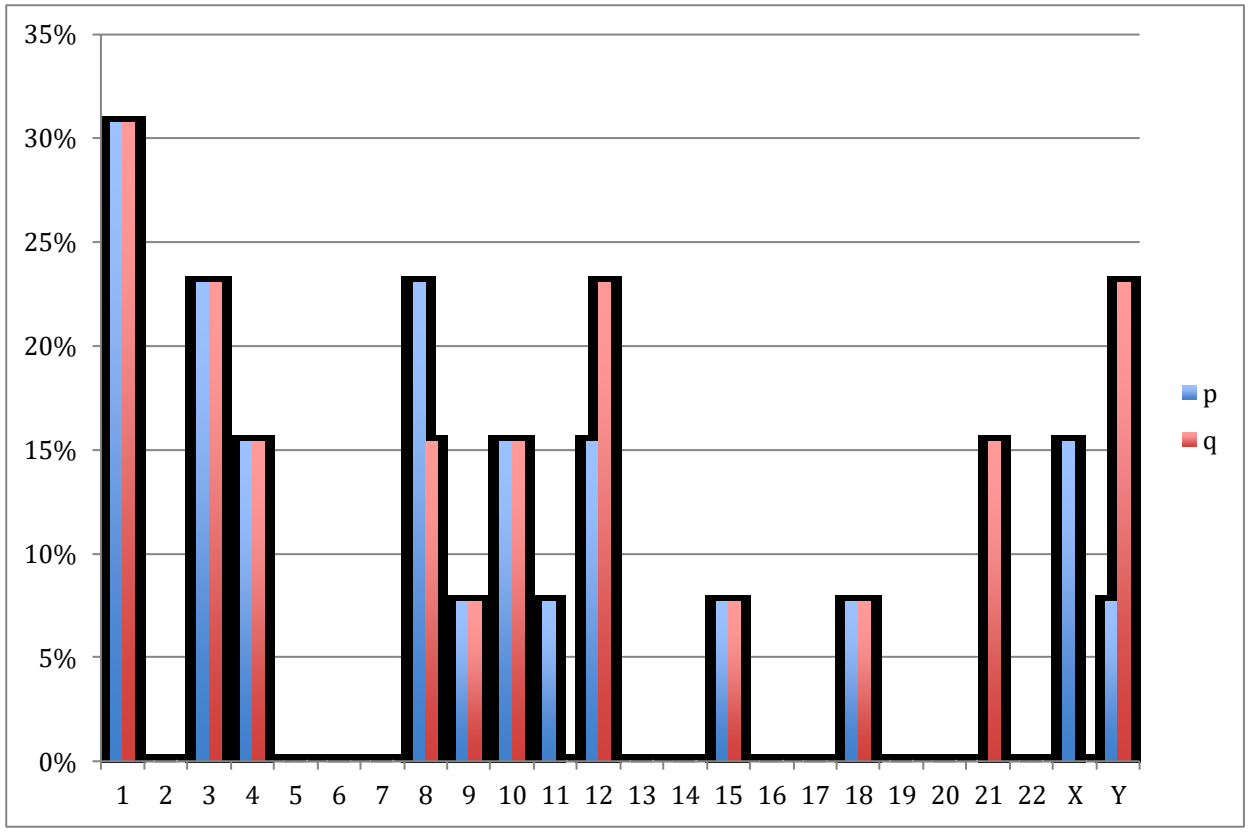

Figure 15: chromosomal loss. The Y axis shows the percentage of patients . The x axis shows the short and long arm loss for each chromosome.

% patients with DNA alterations

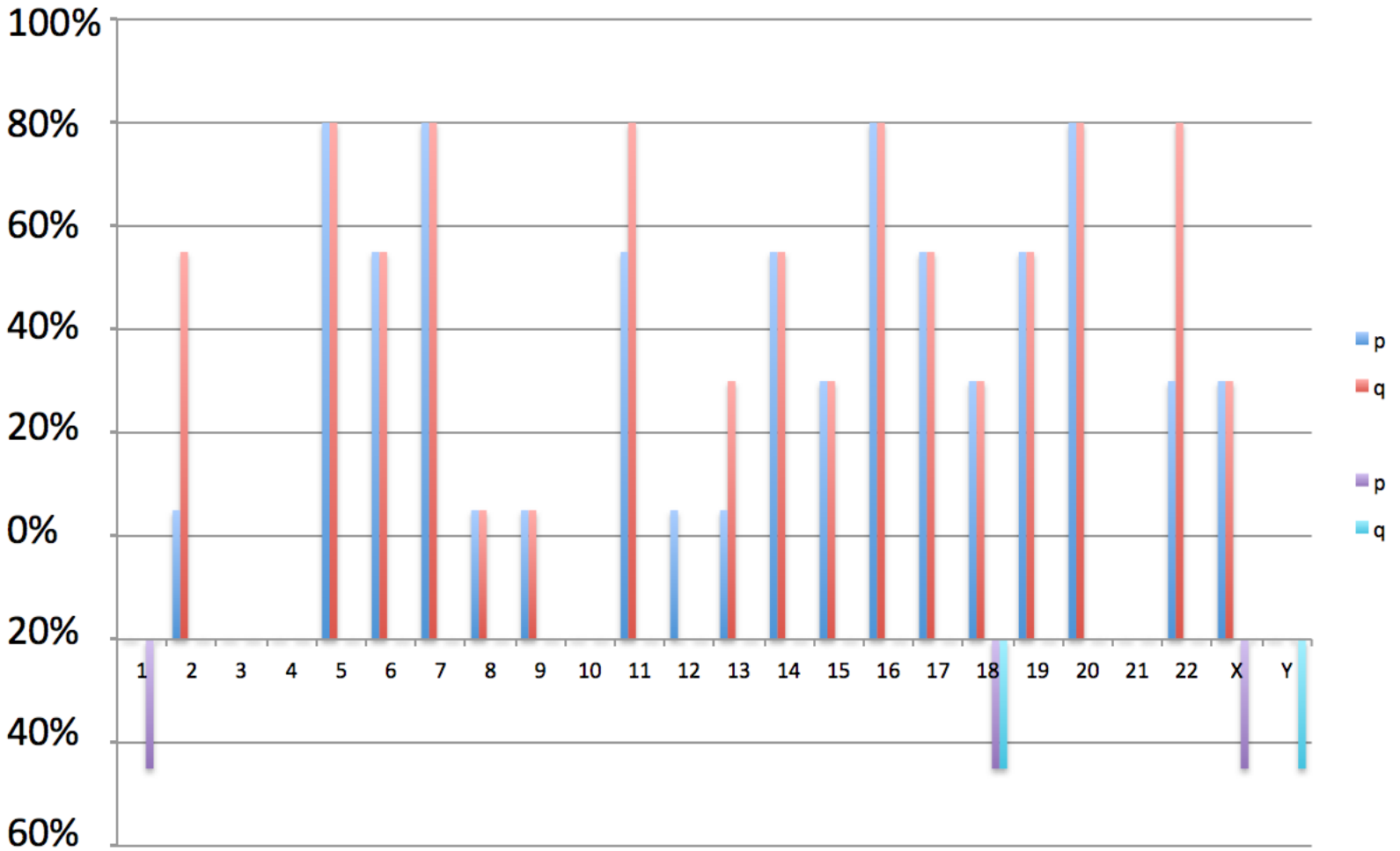

Figure 16: percentage of patients with DNA gain or loss for each chromosome. The Y axis shows the percentage of patients with gain or loss in chromosome. The X axis indicates the chromosome number. **FRESH= tumor tissue obtained during surgery**

	1+	2+	3+	4+	5+	6+	7+	8+	9+	10+	11+	12+	13+	14+	15+	16+	17+	18+	19+	20+	21+	22+	X+	Y+
Pz.1		2p12-2q12.1			pq		pq				pq		q	q	q	pq		pq	pq	pq	q	q	pq	
Pz. 2					pq	pq	pq	8p12-p21.1	pq		q	p	p	p	p	pq	pq	pq		pq		q		
pz.3		pq			pq	pq	pq				11pter-q22.3		pq	pq		pq	pq		pq	pq	21q21.1-21.2	pq		
pz.4		pq			pq	pq	pq				pq			pq	pq	pq	pq		pq	pq	21q21.1-21.2	pq	pq	

Table 13: amplificated regions in fresh tissue samples showed by the a-CGH

	1-	2-	3-	4-	5-	6-	7-	8-	9-	10-	11-	12-	13-	14-	15-	16-	17-	18-	19-	20-	21-	22-	X-	Y-
Pz.1																								q
Pz. 2																								
pz.3	p32.3-13.2																	pter-q12.1					p21.1	
pz.4																								

Table 14: loss regions in fresh tissue samples showed by the a-CGH

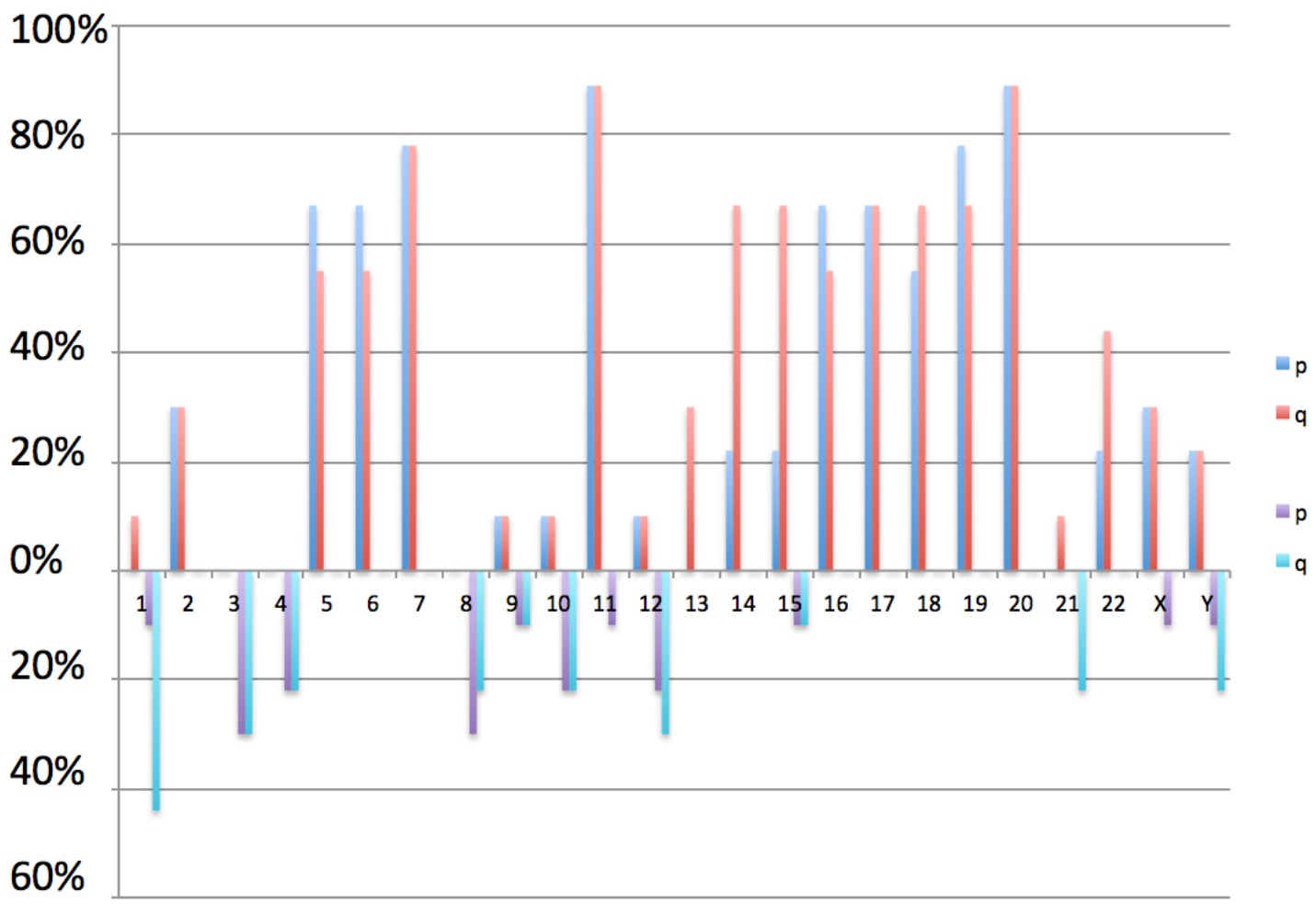
% patients with DNA alterations
100%
80%
60%
40%
20%
0%
20%
40%
60%
1
2
3
4
5
6
7
8
9
10
11
12
13
14
15
16
17
18
19
20
21
22
X
Y
p
q
p
q

Figure 17: percentage of patients with DNA gain or loss for each chromosome. The Y axis shows the percentage of patients with gain or loss in chromosome. The X axis indicates the chromosome number. **FFPE= formalin-fixed and paraffin-embedded tissue samples**

	1+	2+	3+	4+	5+	6+	7+	8+	9+	10+	11+	12+	13+	14+	15+	16+	17+	18+	19+	20+	21+	22+	X+	Y+
Pz.1-P		pq			pq	pq	pq		pq		pq		13q12-13q31.1		q	pq	pq	pq	pq	pq			pq	
PZ.1-R		p			pq	pq	pq				pq													
		q12-2q35																						
		2q36.1-2q36.3																						
Pz.2											pq			q	q			pq	p	pq				
Pz. 3					5p13.3-p14.3	6p21.1-p22.2	7p22.1-pter				11p15.4-pter			14q32.11-qter		16p	pq	18q22.1	19p	20p13-pter	21q22.11-qter	pq		
							7q11.22-22.11				11p11.12-p11.2								9q	20q				
							7q22.1				11q12.2-q14.4													
											11q23.1-qter													
Pz. 4					pq	pq	pq				pq		13q	pq	pq	pq	pq	pq	pq	pq		pq	pq	pq
Pz. 5	1q32.1-q32.2	pq			pq	pq	pq				pq			pq	pq	pq	pq	pq	pq	pq		pq		
Pz. 6																								
pz.7					pq	pq	pq				pq			q	q	pq	pq	pq	pq	pq		q	pq	pq
pz.8							7p21.3-pter		9p13.1-p13.3		11p15.4-pter									pq				
							7qcen-q21.11		9q33.2-qter		11q12.1-14.1													

							7q22.1-q22.2				11q22.3-qter														
pz.9		pq			pq	pq	pq			pq	pq	pq	q	q	q	pq	pq		pq	pq		q		

Table 15: amplificated regions in FFPE tissue samples showed by the a-CGH

	1-	2-	3-	4-	5-	6-	7-	8-	9-	10-	11-	12-	13-	14-	15-	16-	17-	18-	19-	20-	21-	22-	X-	Y-
1-TP	p31.1-p12																							q
	q23.1-q25.1											q24.21												
1-R	p31.1-p12																							
	q23.1-q25.1																							q
2																								
3	1 (complesso)		3 compl	pq				pq	9 compl	pq		12 compl	pq		pq						q21.1-q21.3		p11.4-21.3	
4	q31.1-q32.1		3pcen-p12.3					p23.1-p23.2																
			3q21-q26.2																					
5																								
6																								
7																								
8	pcenp33		pq	pq				pq		pq	11p11.2-p12	p												
	q23.1-qter											qcen-q13.11												
												q14.1-q24.11									q21.1-q22.11			pq
9																								

Table 16: loss regions in FFPE tissue samples showed by the a-CGH

Biases in the results of FFPE samples versus FRESH samples

Formalin-fixed, paraffin embedded (FFPE) tissue samples are a suitable source for such retrospective studies, but there is a valid concern about coupling of array CGH with the use of FFPE specimens, because of the variable deegre of DNA degradation and the oxidative and crosslinkage effect of formalin.

Those crosslinks cause DNA breakage during the extraction process. Another limitation is the small quantity of DNA obtained from often microdissected FFPE lesions. Moreover, the passage of time and the storage condition of FFPE blocks influence the quality of DNA. We used FFPE samples as recent as possible, but we experienced anyway an increase in the deegre of DNA fragmentation and the loss og high molecular weight DNA after extraction that may be observed in the aCGH results. As examples in figure18 it is shown the comparison of the same chromosome 1 between two samples from FFPE (18A and 18B) and one fresh sample (18C). 18A and 18B are the same patient (no.1) where 18A is relative to the onset of the pathology and 18B is the relapse. 18C is a different patient (no.3) at the onset of the pathology. It well evident the moving average profile (that indicates the chromosome imbalances of patient and should be as much linear as possible) in case of FFPE samples shows a fragmented profile, while in the fresh sample it is quite linear. This is due to the DNA integrity and in this case, it is difficult for the ADM2 algorithm of the software to identify the imbalances correctly. In fact, 18A and 18B show the same moving average profile, but in 18A two deep deletion profiles are evidenced by the software, while in 18B, despite the profile of the moving average is the same, only one aberration it is shown.

Figure 19 (A, B and C) is the same figure 18 where also the scattered plot profile is shown. This profile displays a green or red spot for each probe and the localization of the spot is relative to the fuorescence ratio of patient versus reference DNA. A wide distribution of the scattered plots, as can be seen in 19A and 19B, indicates DNA damage, while a tight scattered plot, as in figure 19C, indicates optimal DNA condition.

Despite the problems of DNA damage as may be found in FFPE samples, the entire chromosome aneuploidy are correctly seen (Figure 20, A and B the same patient (no.1, onset and relapse) for the duplication of chromosome 20 and 20C for the fresh sample (no.3). As shown in fig. 18A and 18B the average moving in fig. 20 (A-B) shows a fragmented profile, while for the fresh sample (fig. 20C) the profile is quite linear. In fig. 21 duplication of chromosome 5 is correctly put in evidence in FFPE and FRESH samples.

So, the problem of FFPE samples is only relative to little regions of chromosome imbalances, while for entire chromosome aneuploidy (very frequent in ONB) the problem is less relevant.

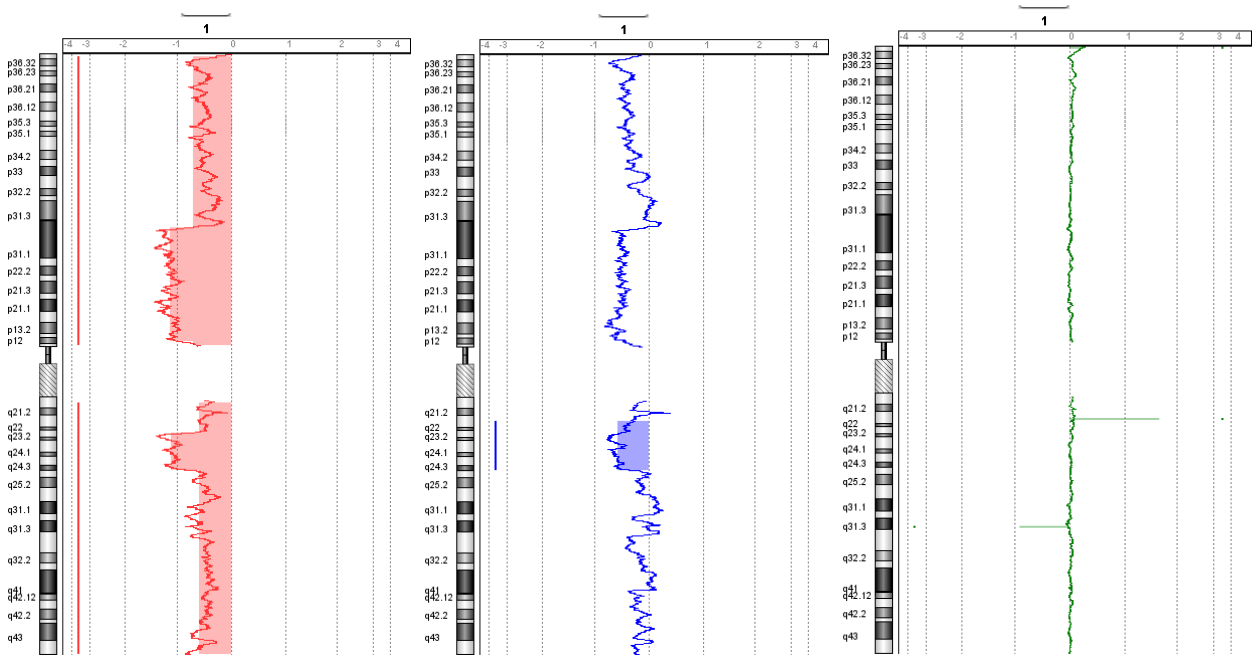

Fig.18 A B C

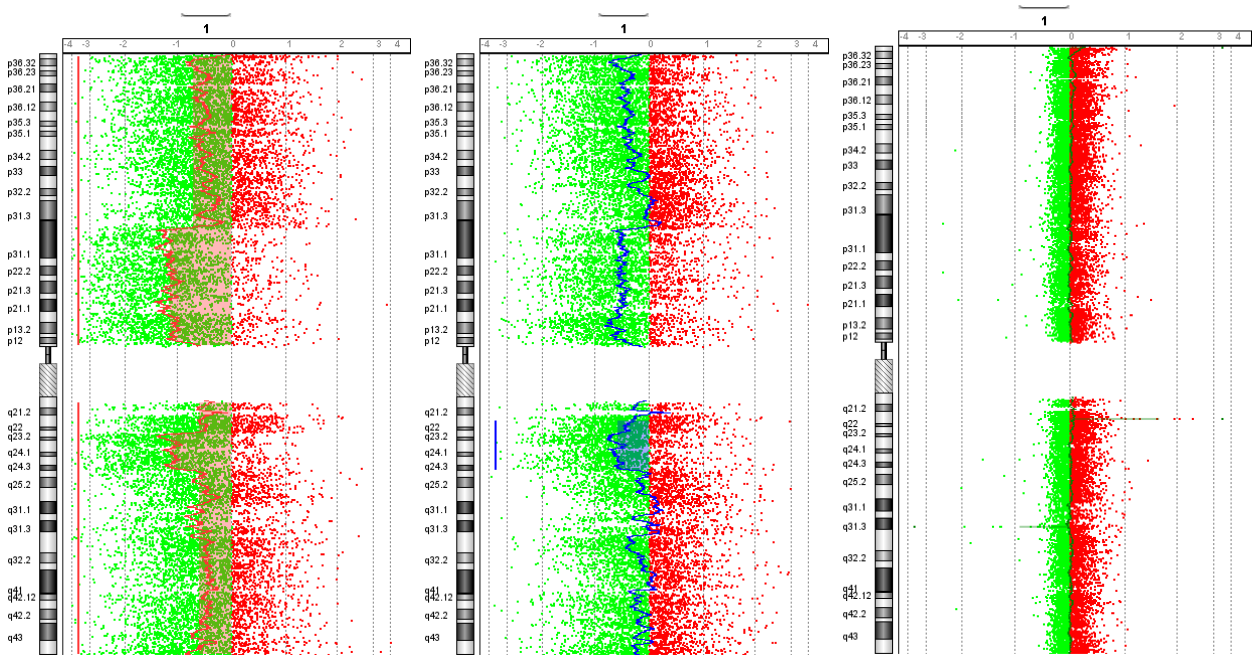

Fig.19 A B C

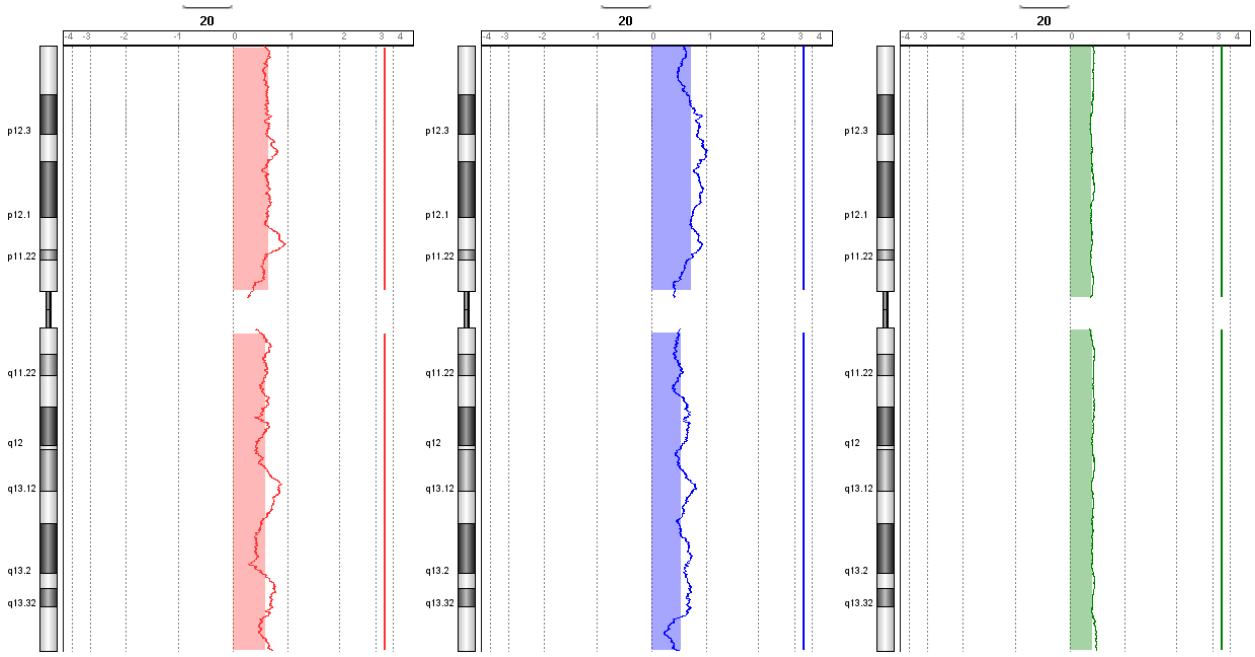

Fig.20 A B C

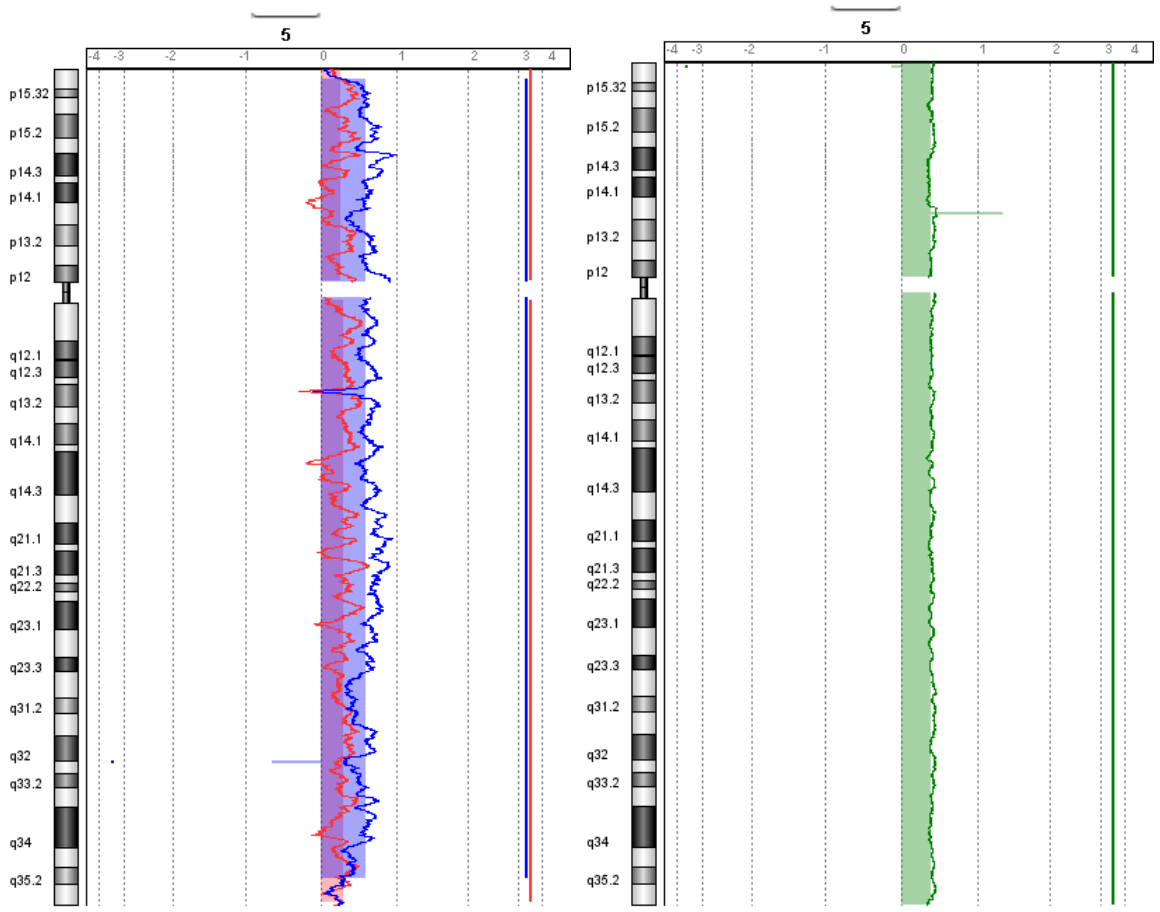

Fig.21 A B

6. Discussion

Olfactory neuroblastoma (ONB) arises from the neural-epithelial olfactory mucosa. The mainstay treatment of ONB generally comprises radical surgical resection[6]. In our experience, surgical excision should include the dura of the ASB together with the ipsilateral olfactory bulb in every case, not only to obtain a free-margins resection of the disease but also for staging purposes[6]. The removal of both olfactory bulbs is performed only for bilaterally extended cancers. Postoperative irradiation has been shown to reduce local recurrence rates and improve survival, so it is recommended in all cases, irrespective of extent of disease at diagnosis[1,47]. Radiation treatment is

typically delivered using IMRT, which provides optimal sparing of radiation dose to sensitive normal structures, such as the optic nerve or brain. The recent introduction of intensity-modulated proton beam radiation therapy (IMPBRT) deserves particular mention, showing promising results for the management of ONB both as exclusive primary therapy and in the postoperative setting[48]. Cervical lymph node metastases are infrequent at presentation for patients diagnosed with ONB, with reported rates between 5% and 12%. However, given the high reported rates of late regional failures and limited morbidity-associated IMRT, elective neck radiation may warrant consideration in patients with intracranial disease at presentation (Kadish C)[1]. Particular attention should be paid to Hyams grading, which accurately characterizes tumor biology and represents an independent predictor of locoregionally recurrence of disease and overall survival (OS)[47]. For this reason, it is a valuable asset to consider when contemplating adjuvant or neoadjuvant therapies. In detail, poorly differentiated ONB, namely Hyams grade IV lesions, presenting in locally advanced stages (T3–T4), could benefit from different regimens of induction chemotherapy (etoposide/cisplatin[49] or cyclophosphamide/vincristine[50,51]) to improve both disease control and survival rates; however, the existing data do not provide any definitive indication in this field.

A-CGH is a relatively new technology designed to allow high throughput screening of chromosomal gains and losses in diseases, particularly cancer.

Cytogenetic data on ONB from literature are scarce and rather sparce; the aim of our study is to identify DNA copy number changes in ONB by aCGH.

We decided to compare our results with those of Guled et al. (2008) [7], who reported a-CGH results obtained on 13 patients, and reviewed all previous reports in the literature. Previous data were based on combined results of conventional chromosome analysis, locus-specific fluorescence in situ hybridization (FISH), multicolor FISH, CGH, and single nucleotide polymorphism (SNP) array techniques. A total of 31 patients were reported in the literature for whom some kind of cytogenetic

data were available. In their patient cohort, Guled et al. indicated several regions that were gained in a significant proportion of cases: 7q11.2, 20q13, 5q34-35, 6p12.3, 10p12.31, and 12q23.1-24.31. They observed recurrent losses in 2q31-37, 5q, 6p, 6q, 18q, 15q11.2-24.1, 15q13.1, 19q12-13, 22q11.1-11.21, 22q11.23, and 22q12.1. Most segmental gains and losses found in our patients were different from the imbalances claimed as recurrent by Guled et al., and the only corresponding data concerned the gain of band 20q13 and the loss of segments of chromosomes 15 and 22 (Table 11-12). Guled et al., however, only reviewed previous data that were useful for a comparison with their own results. Thus, we reanalyzed all available data in the literature[7,40,41,42,43,52] and compared them with our results. We remark, however, that our results and those of Guled et al (2008) identify more precisely the chromosome segments gained and lost in comparison with previous studies. For instance, gains and losses of chromosomes 15 and 20 found in our cases concerned small segments that were similar, but not identical to those previously reported as frequent; in another case, the region lost on chromosome 22 was adjacent, but different from the one already identified. Weiss et al.[52] applied Next Generation Sequencing (NGS) to one patient with ONB, and they precisely identified regions gained or lost. A comparison with our data showed the following similarities: they showed the gain of the short arms of chromosome 8, and we found the gain of the region 8p21.1-21.2 in one patient. They noted the gain of two chromosome 16 regions, 16q22.1 and 16q24.3: similarly, we observed the gain of 16q21-22.2 in one patient and of the entire long arms of chromosome 16 in another subject (Table 11). They reported the loss of 19p12, while we found the loss of 19p11-12 in one patient; they indicated the loss of 21q1, and we found the loss of 21q11.1-21.3 (Table 12). These were the only similar anomalies observed, although the regions involved were not identical. Thus, as far as segmental chromosome imbalances are concerned, it was not possible to make conclusions on real recurrent regions gained or lost, although a high level of chromosome instability was confirmed.

In our cohort, eleven out of 13 samples revealed gains of several entire chromosomes; and no gains

or losses in one patient (Table 11-12). The comparison with literature data is inconsistent, except for the gain of chromosome 19, present in 10/14 of our samples and in 3/3 patients reported by Riazimand et al.[41]. Otherwise, few gains and losses of entire chromosomes have been reported.

Of interest, in patient no.1 a comparison of the primary and relapsed tumor showed a clonal evolution. The number of trisomies was reduced, while several segmental gains were added, and segmental losses were identical except for 10q25.1 (Table 11-12).

Archived FFPE specimens allow for the retrospective study of a large number of cases but are limited by potentially suboptimal DNA quality.

PCR amplicon size and storage period were key factors influencing the success rate of DNA extraction from FFPE samples. Another major factor affecting the DNA quality is the presence of necrosis in tissue specimens. It is likely that the adverse effect of necrosis is due to the DNA degradation of necrotic cells. However, such DNA degradation contributed by necrosis could not be revealed by PCR-based assessment of DNA integrity, as it would be masked by the relatively intact DNA from 'viable' cells[53,54,55,56]. However, necrosis is easily identified by histological review and its adeverse effect on aCGH can be eliminated by microsdissection[57]. In line with loss of eterozygosity analysis, sensitivity of aCGH in detection of DNA copy number changes heavily depends on the proportion of tumor cells in a tissue specimen. Together with the adverse effect of necrosis, this emphasises the importance of routine histological review of tissue specimens selected for aCGH[58].

In the fresh-frozen samples, the DNA extraction success rate was 100% using either a commercial kit (QIAamp DNA Micro) or a laboratory based method regardless of PCR amplicon length or tissue storage time[59].

Our results show how the problem of quality of aCGH of FFPE samples is principally relative to the identification of little regions of chromosome imbalances, while for entire chromosome aneuploidy, that are very frequent in olfactory neuroblastomas, the problem is less relevant. Undoubtedly we

can conclude that the optimal method for DNA extraction and for aCGH analysis is the use of fresh-frozen samples.

Our efforts to identify important chromosome imbalances in ONB pathogenesis and disease course are largely inconclusive: no specific segmental chromosome anomalies were consistently present in a significant proportion of the tumors. We were not able to confirm most of the conclusions. The exceptions were frequent gain of chromosome 19, gain of some regions of the long arm of 20, while some regions of the long arm of 22 were often lost. Our data do not indicate a correlation between imbalances and Kadish stage or Hyams' grade.

However these preliminary results, although obtained in only 13 patients, demonstrated that the a-CGH is a tool of fundamental importance in the study of cytogenetic abnormalities in solid tumors.

Therefore the results obtained in our study, could contribute in the future to better define the cytogenetic profile of ONB , to identify possible correlations with clinical and pathological features and also to find targeted therapeutic protocols.

A-CGH will require further analysis based on larger series to determine the role of the regions identified in ONB and to validate these preliminary results of our study.

7. REFERENCES

1. Dulguerov P, Calcaterra M: Esthesioneuroblastoma: The UCLA Experience 1970-1990. *Laryngoscope* 102: 843-848, 1992.
2. Dulguerov P, Allal AS, Calcaterra TC. Esthesioneuroblastoma: a meta-analysis and review. Lancet Oncol 2001;2:683–690. [PubMed: 11902539

3. Broich G, Pagliari A, Ottavini F: Esthesioneuroblastoma: A General Review of the Cases Published Since the Discovery of the Tumour in 1924. *Anticancer Research* 17: 2683-2706.
4. Bradley PJ, Jones NS, Robertson I. Diagnosis and management of esthesioneuroblastoma. Curr Opin Otolaryn- gol Head Neck Surg 2003;11:112–118.
5. Castelnuovo P, Battaglia P, Locatelli D et al. Endonasal micro-endoscopic treatment of the malignant tumours of paranasal sinuses and anterior skull base. *Operative Techniques in Otolaryngology.* 17(3):152-167, 2006.
6. Castelnuovo P, Bignami M, Delù G, Battaglia P, Bignardi M, Dallan I: Endonasal endoscopic resection and radiotherapy in olfactory neuroblastoma: our experience. *Head & Neck* Sep;29(9):845-50, 2007.
7. Guled M, Myllykangas S, Frierson HF Jr, et al. Array comparative genomic hybridization analysis of olfactory neuroblastoma. Mod Pathol. 2008;21:770–778.
8. Berger RL, Luc R: l´esthesioneuroepitheliome Olfactif. *Bull Assoc Franc Pour L´etude Cancer* 13 : 410-420, 1924.
9. Pickuth D, Heywang-Köbrunner SH: Imaging of Recurrent Esthesioneuroblastoma. *The British Journal of Radiology* 72: 1052-1057, 1999.
10. Pickuth D, Heywang-Köbrunner SH: Imaging of Recurrent Esthesioneuroblastoma. *The British Journal of Radiology* 72: 1052-1057, 1999
11. Kadish S, Goodman M, Wang CC: Olfactory Neuroblastoma, a Clinical Analysis of 17 Cases. *Cancer* 37: 1571-1576, 1976.
12. Koka VN, Julieron M, Bourhis J, Janot F, Le Ridant AM, Marandas P, Luboinski B, Schwaab G. Aesthesioneuroblastoma. J Laryngol Otol. 1998 Jul;112(7):628-33.
13. Miyamoto RC, Gleich LL, Biddiger PW, Gluckman JL: Esthesioneuroblastoma and Sinonasal Undifferentiated Carcinoma: Impact of Histological Grading and Clincal Staging on Survival and Prognosis. *Laryngoscope* 110: 1262-1265, 2000

14. Ogura JH, Schenck NL. Unusual nasal tumours. Problems in diagnosis and treatment. Otolaryngologic Clinics of North America 1973;6 (3):813-37
15. Hirose T, Scheithauer BW, Lopes MB, Gerber HA, Altermatt HJ, Harner SG, et al. Olfactory neuroblastoma. An immunohistochemical, ultrastructural, and flow cytometric study. Cancer 1995;76(1):4-19.
16. Resto VA, Eisele DW, Forastiere A, Zahurak M, Lee DJ, Westra WH. Esthesioneuroblastoma: the Johns Hopkins experience. Head & Neck 2000;22(6):550-8.
17. Hyams VJ, Batsakis JG, Michaels L. Tumours of the upper respiratory tract and ear. Armed Forces Institute of Pathology Fascicles, 2nd series. Washington : American Registry of Pathology Press; 1988.
18. Foote RL, Morita A, Ebersold MJ, Olsen KD, Lewis JE, Quast LM, et al. Esthesioneuroblastoma: the role of adjuvant radiation therapy. International Journal of Radiation Oncology, Biology, Physics 1993;27(4):835-42.
19. Koch M, Constantinidis J, Dimmler A, Strauss C, Iro H. [Longterm experiences in the therapy of esthesioneuroblastoma].Laryngo- Rhino- Otologie 2006;85(10):723-30.
20. Rastogi M, Bhatt M, Chufal K, Srivastava M, Pant M, Srivastava K, et al. Esthesioneuroblastoma treated with non-craniofacial resection surgery followed by combined chemotherapy and radiotherapy: An alternative approach in limited resources. Japanese Journal of Clinical Oncology 2006;36(10):613-9.
21. Biller HF, Lawson W, Sachdev VP, Som P. Esthesioneuroblastoma: surgical treatment without radiation. Laryngoscope 1990;100(11):1199-201.
22. Morita A, Ebersold MJ, Olsen KD, Foote RL, Lewis JE, Lynn MQ: Esthesioneuroblastoma: Prognosis and Management. *Neurosurgery* 32: 706-715, 1993
23. Lund VJ, Howard D, Wei W, Spittle M. Olfactory neuroblastoma: past, present, and future? Laryngoscope 2003;113:502–507. [PubMed: 12616204

24. Lund VJ, Stammberger H, Nicolai P, Castelnuovo P, Beale T, Beham A, Bernal-Sprekelsen M, Braun H, Cappabianca P, Carrau R, Clarici G, Draf W, Esposito F, Fernandez-Miranda J, Fokkens WJ, Gardner P, Gellner V, Hellquist H, Hermann P, Hosemann W, Howard D, Jones N, Jorissen M, Kassam A, Kelly D, Kurschel-Lackner S, Leong S, McLaughlin N, Maroldi R, Minovi A, Mokry M, Onerci M, Ong YK, Prevedello D, Saleh H, Sehti DS, Simmen D, Snyderman C, Solares A, Spittle M, Stamm A, Tomazic P, Trimarchi M, Unger F, Wormald PJ, Zanation A. European position paper on endoscopic management of tumours of the nose, paranasal sinuses and skull base. Rhinology 2010;48(Suppl 22):46–51.
25. Carta F, Kania R, Sauvaget E, Bresson D, George B, Herman P. Endoscopic skull base resection for adenocarcinoma and olfactory neuroblastoma. Rhinology. In press 2010.
26. Castelnuovo P: La dissezione anatomica endoscopica del distretto rino-sinusale – Il training anatomo-chirurgico per le tecniche di base della chirurgia endoscopica rino-sinusale. Editore Endo-Press, Tuttlingen, Germania, 2001.
27. Castelnuovo PG, Delu G, Sberze F, Pistochini A, Cambria C, Battaglia P, et al. Esthesioneuroblastoma: endonasal endoscopic treatment. Skull Base: An Interdisciplinary Approach 2006;16(1):25-30.
28. Devaiah AK, Andreoli MT. Treatment of esthesioneuroblastoma: a 16-year meta-analysis of 361 patients. Laryngoscop 2009;119(7):1412-6.
29. Folbe A, Herzallah I, Duvvuri U, Bublik M, Sargi Z, Snyderman CH, Carrau R, Casiano R, Kassam AB, Morcos JJ. Endoscopic endonasal resection of esthesioneuroblastoma: a multicenter study. Am J Rhinol Allergy. 2009 Mar-Apr;23(2):238.
30. Eich HT, Staar S, Micke O, Eich PD, Stützer H, Müller RP: Radiotherapy of Esthesioneuroblastoma. *Head and Neck* 49: 155-160, 2001.
31. Mc Elroy EA, Buckner JC, Lewis JE: Chemotherapy for Advanced Esthesioneuroblastoma: The Mayo Clinic Experience. *Neurosurgery* 42: 1023-1028, 1998.

32. Polin RS, Sheehan JP, Chenelle AG, Munoz E, Larner J, Phillips CD, et al. The role of preoperative adjuvant treatment in the management of esthesioneuroblastoma: the University of Virginia experience. Neurosurgery 1998;42(5):1029-37.
33. Kallioniemi A, Kallioniemi OP, Sudar D, et al. Comparative genomic hybridization for molecular cytogenetic analysis of solid tumours. Science 1992; 258: 818-21
34. Albertson DG. Profiling breast cancer by array CGH. Breast Cancer Res Treat 2003; 78:289-98
35. Pinkel D, Segraves R, Sudar D, et al. Quantitative high resolution analysis of DNA copy number variation in breast cancer using comparative genomic hybridization to DNA microarrays. Nat Genet 1998; 20:207-11
36. Gilbert N, Boyle S, Fiegler H, Woodfine K, Carter NP, Bickmore WA: Chromatin architecture of the human genome: gene-rich domains are enriched in open chromatin fibers. Cell 2004, 118:555–566
37. Gitan RS, Shi H, Chen CM, Yan PS, Huang TH: Methylation-specific oligonucleotide microarray: a new potential for high-throughput methylation analysis. Genome Res 2002, 12:158–164
38. Vissers LE, van Ravenswaaij CM, Admiraal R, Hurst JA, de Vries BB, Janssen IM, van der Vliet WA, Huys EH, de Jong PJ, Hamel BC, Schoenmakers EF, Brunner HG, Veltman JA, van Kessel AG: Mutations in a new member of the chromodomain gene family cause CHARGE syndrome. Nat Genet 2004, 36:955–957
39. Hyams VJ: Tumours of the Upper Respiratoy Tract and Ear. In: Hyams VJ, Batsakis JG, Michaels L, eds. *Atlas of Tumour Pathology.* 2nd series, Fascicle 25. Washington, DC: Armed Forces Institute of Pathology, 1988, p. 240-248.
40. Szymas J, Wolf G, Kowalczyk D, Nowak S, Petersen I: Olfactory Neuroblastoma: Detection of Genomic Imbalances by Comparative Genomic Hybridization. *Acta Neurochir (Wien)* 139: 839-844.

41. Riazimand SH, Brieger J, Jacob R, et al. Analysis of cytogenetic aberrations in esthesioneuroblastomas by comparative genomic hybridization. Cancer Genet Cytogenet. 2002; 136:53–57
42. Bockmühl U, You X, Pacyna-Gengelbach M, Arps H, Draf W, Petersen I. CGH pattern of esthesioneuroblastoma and their metastases. *Brain Pathol.* Apr;14 (2):158-63, 2004
43. Holland H, Koschny R, Krupp W, Meixensberger J, Bauer M, Kirsten H, Ahnert P. Comprehensive cytogenetic characterization of an esthesioneuroblastoma. Cancer Genet Cytogenet. 2007 Mar;173 (2):89-96.
44. Faragalla H, Weinreb I. Olfactory neuroblastoma: a review and update. Adv Anat Pathol 2009;16: 322–331
45. Furlan D, Cerutti R, Genasetti A, Pelosi G, Uccella S, La Rosa S, Capella C. 2003. Microallelotyping defines the monoclonal or the polyclonal origin of mixed and collision endocrine-exocrine tumors of the gut. Lab Invest 83:963–971
46. Valli R, Maserati E, Marletta C, Pressato B, Lo Curto F, Pasquali F. 2011. Evaluating chromosomal mosaicism by array comparative genomic hybridization in haematological malignancies: The proposal of a formula. Cancer Genet 204:216–218.
47. Ow TJ, Hanna EY, Roberts DB, et al. Optimization of long-term outcomes for patients with esthesioneuroblastoma. Head Neck 2014;36(4):524–30.
48. Nishimura H, Ogino T, Kawashima M, et al. Proton-beam therapy for olfactory neuroblastoma. Int J Radiat Oncol Biol Phys 2007;68(3):758–62.
49. Van Gompel JJ, Giannini C, Olsen KD, et al. Long-term outcome of esthesioneuroblastoma: Hyams grade predicts patient survival. J Neurol Surg B Skull Base 2012;73(5):331–6.
50. Chao KS, Kaplan C, Simpson JR, et al. Esthesioneuroblastoma: the impact of treatment modality. Head Neck 2001;23(9):749–57.

51. Mitchell EH, Diaz A, Yilmaz T, et al. Multimodality treatment for sinonasal neuroendocrine carcinoma. Head Neck 2012;34(10):1372–6.

52. Weiss GJ, Liang WS, Izatt T, Arora S, Cherni I, Raju RN, Hostetter G, Kurdoglu A, Christoforides A, Sinari S, Baker AS, Metpally R, Tembe WD, Phillips L, Von Hoff DD, Craig DW, Carpten JD. 2012. Paired tumor and normal whole genome sequencing of metastatic olfactory neuroblastoma. PloS One 7: e37029. doi:10.1371/journal.pone.0037029

53. Andreassen CN, Sorensen FB, Overgaard J, Alsner J. Optimisation and validation of methods to assess single nucleotide polymorphisms (SNPs) in archival histological material. Radiother Oncol 2004, 72: 351–356

54. Ferrer I, Armstrong J, Capellari S, Parchi P, Arzberger T, Bell J, et al. Effects of formalin fi xation, paraffi n embedding, and time of storage on DNA preservation in brain tissue: a BrainNet Europe study. Brain Pathol 2007, 17: 297–303

55. Matevossian A, Akbarian S. Neuronal nuclei isolation from human postmortem brain tissue. J Vis Exp 2008, (20): e914. doi:10.3791/914.

56. Huang HS, Matevossian A, Jiang Y, Akbarian S. Chromatin immunoprecipitation in postmortem brain. J Neurosci Methods 2006, 156: 284–292.

57. Jackson DP, Lewis FA, Taylor GR, Boylston AW, Quirke P. Tissue extraction of DNA and RNA and analysis by the polymerase chain reaction. J Clin Pathol 1990, 43: 499–504.

58. Schiffner LA, Bajda EJ, Prinz M, Sebestyen J, Shaler R, Caragine TA. Optimization of a simple, automatable extraction method to recover sufficient DNA from low copy number DNA samples for generation of short tandem repeat profi les. Croat Med J 2005, 46: 578–586

59. Cotter FE, Hall PA, Young BD. Extraction of DNA from small sections of frozen tissue with simultaneous histological examination. J Clin Pathol 1988, 41: 1125–1126